Int J Earth Sci (Geol Rundsch) (2014) 103:61–82
DOI 10.1007/s00531-013-0941-1

ORIGINAL PAPER

Basement lithostratigraphy of the Adula nappe: implications for Palaeozoic evolution and Alpine kinematics

Mattia Cavargna-Sani · Jean-Luc Epard · François Bussy · Alex Ulianov

Received: 6 March 2013 / Accepted: 8 July 2013 / Published online: 20 August 2013

Abstract The Adula nappe belongs to the Lower Penninic domain of the Central Swiss Alps. It consists mostly of pre-Triassic basement lithologies occurring as strongly folded and sheared gneisses of various types with mafic boudins. We propose a new lithostratigraphy for the northern Adula nappe basement that is supported by detailed field investigations, U–Pb zircon geochronology, and whole-rock geochemistry. The following units have been identified: Cambrian clastic metasediments with abundant carbonate lenses and minor bimodal magmatism (Salahorn Formation); Ordovician metapelites associated with amphibolite boudins with abundant eclogite relicts representing oceanic metabasalts (Trescolmen Formation); Ordovician peraluminous metagranites of calc-alkaline affinity ascribed to subduction-related magmatism (Garenstock Augengneiss); Ordovician metamorphic volcanic–sedimentary deposits (Heinisch Stafel Formation); Early Permian post-collisional granites recording only Alpine orogenic events (Zervreila orthogneiss). All basement lithologies except the Permian granites record a Variscan + Alpine polyorogenic metamorphic history. They document a complex Paleozoic geotectonic evolution consistent with the broader picture given by the pre-Mesozoic basement framework in the Alps. The internal consistency of the Adula basement lithologies and the stratigraphic coherence of the overlying Triassic sediments suggest that most tectonic contacts within the Adula nappe are pre-Alpine in age. Consequently, mélange models for the Tertiary emplacement of the Adula nappe are not consistent and must be rejected. The present-day structural complexity of the Adula nappe is the result of the intense Alpine ductile deformation of a pre-structured entity.

Keywords Adula nappe · Central Alps · Palaeozoic basement · U–Pb dating · Zircon

Introduction

Palaeozoic basement rocks in the Alpine realm experienced a complex pre-Mesozoic geological evolution, which has generated major lithostratigraphic unconformities. These structures are relatively easy to distinguish from those resulting from the Alpine orogeny in the external parts of the Alpine belt because pre-Mesozoic structures were mostly formed under high-grade metamorphic conditions, whereas Alpine structures developed under low-grade metamorphic conditions. The situation is much more confusing in the internal parts of the Alpine belt because both pre- and post-Mesozoic tectonic structures formed under high-grade conditions. There is thus a potential risk in ascribing pre-Mesozoic features to Alpine events, which may lead to erroneous tectonic interpretations. The best way to avoid such cases is to identify internally consistent lithologic formations within the Alpine basement, which will document its Paleozoic geodynamic evolution.

The Alpine domain is composed in part by nappes made of Palaeozoic basement. Nappes of this type occur in the Lepontine dome. The nappes of the Lepontine dome are mainly assigned to Lower Penninic structural domain. Their Paleogeographic position prior to the Alpine orogenesis is the distal European margin. The Lepontine dome

Electronic supplementary material The online version of this article (doi:10.1007/s00531-013-0941-1) contains supplementary material, which is available to authorized users.

M. Cavargna-Sani (✉) · J.-L. Epard · F. Bussy · A. Ulianov
Institut des Sciences de la Terre, Bâtiment Géopolis, Université de Lausanne, 1015 Lausanne, Switzerland
e-mail: mattia.cavargna-sani@unil.ch

represents a structural and metamorphic dome and includes the deepest nappes of the Alpine edifice. Consequently these nappes are mainly formed by Palaeozoic basement rocks affected by a strong Alpine metamorphism and deformation.

The Adula nappe, in the Central Alps, is a good example of a complexly structured polyorogenic unit and is a key tectonic unit located at the transition between the Helvetic and Briançonnais domains. It is mostly composed of Paleozoic basement rocks and has been strongly deformed by Alpine orogenic events. Various interpretations have led to contrasting kinematic models of its Alpine evolution in the literature.

The Adula nappe is located on the border of the Swiss-Italian Alps on the eastern Lepontine dome and is one of the highest units of the Lower Penninic basement nappe stack (Fig. 1). It is overthrust by the Bündnerschiefer (Gansser 1937; Schmid et al. 1996), a sedimentary series deposited in the North Penninic basin (Steinmann 1994) and followed upward by the easternmost Middle Penninic Tambo and Suretta basement nappes with their associated sediments of Briançonnais affinity. The Adula nappe has been the subject of numerous recent publications and a recent review paper by Nagel (2008); it can be considered one of the best-studied nappes of the Central Alps. The overall structure of the Adula nappe is a north-facing recumbent fold, but its internal structure, which records several deformation phases, is much more complex than that of a simple fold-nappe and contains several slices of Mesozoic rocks folded within the basement (Jenny et al. 1923; Nagel et al. 2002a). The oldest Alpine deformation phases are only locally observable. The dominant Alpine structure in the northern part of the nappe is called the Zapport phase (Löw 1987; Nagel et al. 2002a); it is also the oldest recorded pervasive phase. This phase is associated with the regional foliation, isoclinal folding with approximately N–S fold axes, and a well-marked N–S-stretching lineation associated with a top-to-the-North sense of shear. The Leis and Carassino deformation phases (Löw 1987) are younger and more pronounced in the western part of the northern Adula nappe. The Leis phase is principally expressed by folds, which are locally associated with a cleavage. Large open folds are ascribed to the Carassino phase.

Eclogites and eclogitic facies metapelites are well known in numerous areas of the Adula nappe (Heinrich 1983; Meyre et al. 1999; Dale and Holland 2003; Zulbati 2010). They have been studied mostly in the polymetamorphic basements. The Adula nappe was subject to high-pressure metamorphic conditions during the Alpine orogeny as demonstrated by the metamorphic overprint observed in Mesozoic cover rocks (Zulbati 2008) and the dating of two metamorphic events (the last one being of Alpine age) in eclogites (Herwartz et al. 2011). Alpine decompression and a general Barrovian metamorphism in the Lepontine dome resulted in amphibolite facies conditions in the south and greenschist facies conditions in the northern part of the Adula nappe (Nagel et al. 2002b). Eclogite facies assemblages are restricted to eclogites, garnet–phengite–metapelite, and garnet peridotite (only in the southern part). They are more abundant in the eastern part of the northern Adula nappe.

The pre-Alpine paleogeographic position of the Adula nappe is at the limit of the distal Helvetic margin (Steinmann 1994; Galster et al. 2012), close to the North Penninic basin. The Triassic and Jurassic stratigraphy of the Adula nappe and its surrounding nappes show a transition between the Briançonnais domain and the Helvetic domain (Galster et al. 2012). The limited occurrence of eclogite relicts in a few formations and the strong internal deformation are the main arguments that led several authors to introduce a "lithospheric mélange" model to explain the geometry and kinematics of the Adula nappe (Trommsdorff 1990; Berger et al. 2005). This hypothesis implies that the Adula nappe is a mélange representing the suture between Lower and Middle Penninic (Engi et al. 2001; Berger et al. 2005). This hypothesis remains controversial (see discussion in Herwartz et al. 2011).

The petrographic subdivisions of the Adula nappe were defined in a few classical papers (i.e. Jenny et al. 1923; Kündig 1926; Van der Plas 1959; Egli 1966). A clear lithostratigraphic sequence, however, was never established, and the granitic rocks are still undated. Hence, a consistent picture of the Adula basement architecture, also essential to unravel the Alpine structures, was never proposed.

This work thus aims to:

- determine the protolith of the northern Adula basement rocks;
- date the magmatic protoliths of the northern Adula nappe;
- propose a lithostratigraphy for the Alpine basement rocks;
- suggest a paleogeographic scenario for the protolith formation;
- identify information regarding the pre-Alpine orogenic cycles;
- discuss the implications of the pre-Alpine unconformities in the Alpine kinematics.

Obtaining an accurate lithostratigraphy is essential to conduct a reliable geological and structural map and is of primary importance for the understanding of the nappe kinematics and its metamorphic evolution. This work combines analytical and precise field investigations to constrain the nature of the protoliths of the northern Adula

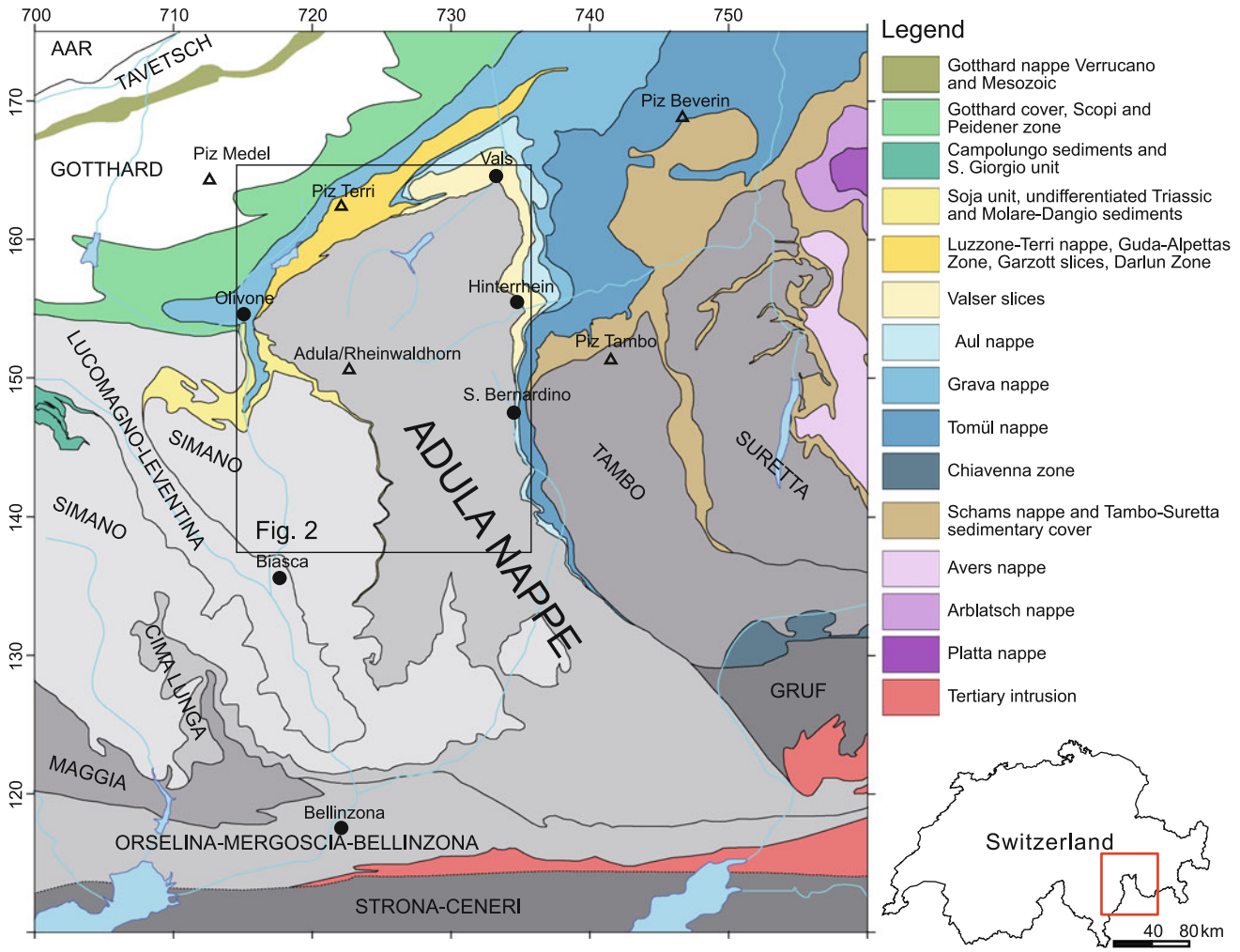

Fig. 1 Tectonic map of the eastern Lepontine Alps. *Grey* and *white* tones are basement nappes, and sediments are illustrated with *colours*. Modified based on the work of Spicher (1980), Berger and Mercolli (2006), Steck (2008), and Galster et al. (2012). The *square* indicates the emplacement of Fig. 2 and the study area. The coordinates represent the kilometric Swiss grid (CH 1903)

nappe rocks and to propose a complete basement lithostratigraphy. Magmatic ages were determined through U–Pb LA-ICPMS dating of zircon. The geodynamic interpretation is supported by whole-rock geochemistry. The proposed new geological map of the northern Adula (Fig. 2) is a combination of the new results from this study and existing geological data. This work is restricted to the northern part of the nappe because it is less metamorphosed and deformed.

Lithology of the northern Adula nappe

Introduction

The names used for the metasedimentary formations and magmatic bodies are as consistent as possible with those used in the literature. The term "Formation" is used to define a lithologically homogeneous body of rock that can be mapped at the 1:25,000 scale. The local names for new Formations are chosen from a well-outcropping area and are shown on the geologic map (Fig. 2).

The rocks described in the following sections underwent one or more metamorphic events and are highly strained. From a geochemical point of view, their content of mobile elements has most likely been modified. For example, some samples of the Garenstock Augengneiss (MC 219, MC 227, MC 272, and MC 302; Online Resource 2) show clear evidence of weathering, which is marked by anomalous values of K_2O, Na_2O, CaO, Sr, Ba, and Pb content. This alteration is most likely due to surface weathering during the pre-Triassic emersion, as suggested by the presence of calcrete and dolocrete under Triassic quartzites ("Adula nappe cover" section). The classification of Pearce (1996; modified after Winchester and Floyd 1977) was chosen to classify mafic rocks because it is based on the

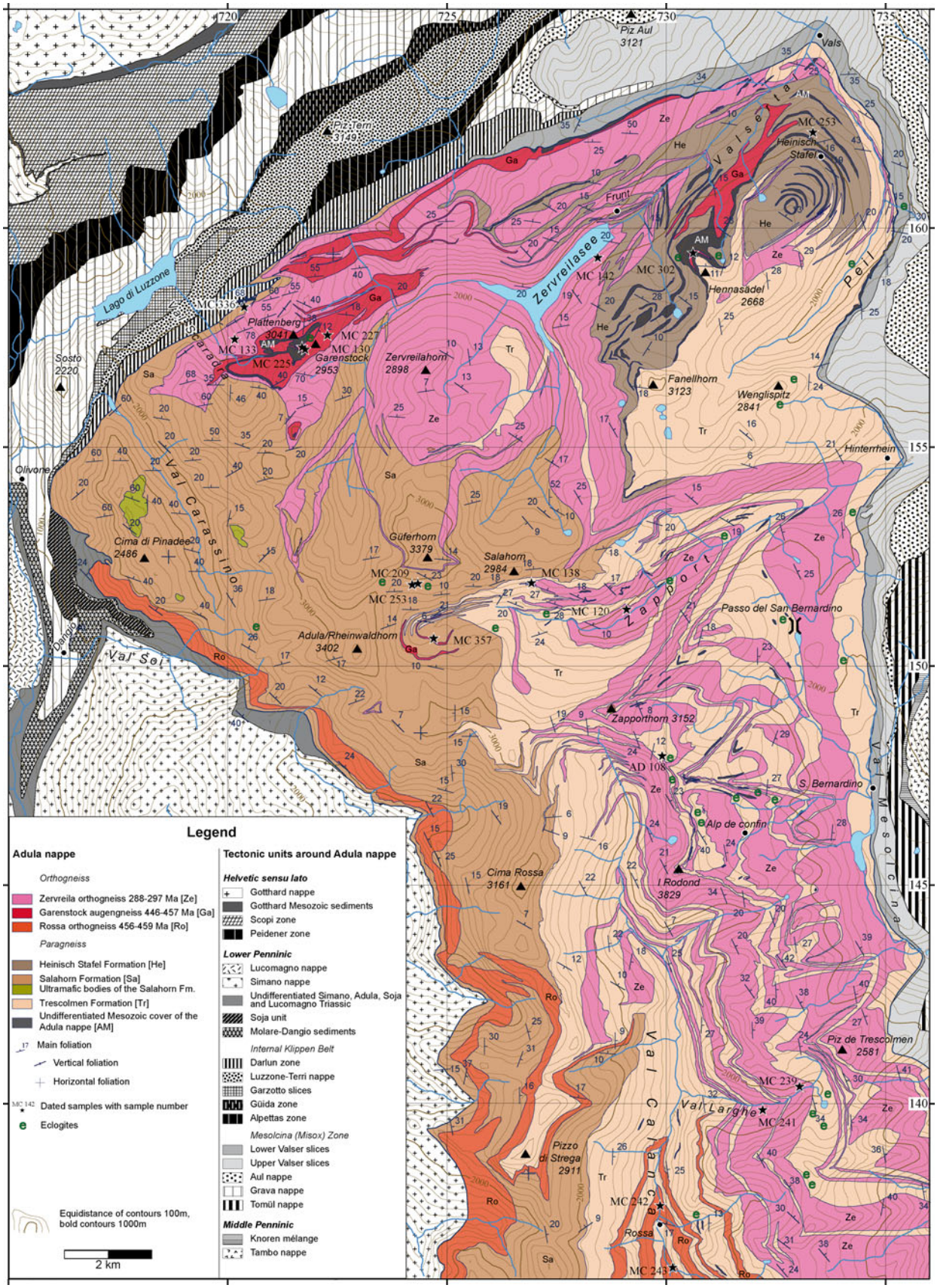
Legend
Adula nappe
Orthogneiss
Zervreila orthogneiss 288-297 Ma [Ze]
Garenstock augengneiss 446-457 Ma [Ga]
Rossa orthogneiss 456-459 Ma [Ro]
Paragneiss
Heinisch Stafel Formation [He]
Salahorn Formation [Sa]
Ultramafic bodies of the Salahorn Fm.
Trescolmen Formation [Tr]
Undifferentiated Mesozoic cover of the Adula nappe [AM]
Main foliation
Vertical foliation
Horizontal foliation
Dated samples with sample number
Eclogites
Equidistance of contours 100m, bold contours 1000m
2 km
Tectonic units around Adula nappe
Helvetic sensu lato
Gotthard nappe
Gotthard Mesozoic sediments
Scopi zone
Peidener zone
Lower Penninic
Lucomagno nappe
Simano nappe
Undifferentiated Simano, Adula, Soja and Lucomagno Triassic
Soja unit
Molare-Dangio sediments
Internal Klippen Belt
Darlun zone
Luzzone-Terri nappe
Garzotto slices
Güida zone
Alpettas zone
Mesolcina (Misox) Zone
Lower Valser slices
Upper Valser slices
Aul nappe
Grava nappe
Tomül nappe
Middle Penninic
Knoren mélange
Tambo nappe
Piz Aul 3121
Vals
Heinisch Stafel
Frunt
Lago di Luzzone
Plattenberg 3041
Garenstock 2953
Zervreilahorn 2898
Zervreilasee
Hennasadel 2668
Fanellhorn 3123
Wenglispitz 2841
Hinterrhein
Sosto 2220
Olivone
Cima di Pinadee 2486
Güferhorn 3379
Salahorn 2984
Adula/Rheinwaldhorn 3402
Passo del San Bernardino
Zapporthorn 3152
S. Bernardino
Alp de confin
Cima Rossa 3161
I Rodond 3829
Piz de Trescolmen 2581
Pizzo di Strega 2911
Rossa
Val Soi
Val Carassino
Val Zapport
Val Mesolcina
Val Curciusa
Val Larghe
Peil

◀ **Fig. 2** Geologic map of the northern Adula nappe. Compilation after Jenny et al. (1923), Künding (1926), Van der Plas (1959), Egli (1966), Frey (1967), Pleuger et al. (2003), Berger and Mercolli (2006), Arnold et al. (2007), Cavargna-Sani (2008), Galster et al. (2010), and Swisstopo (2012), and new mapped area by Cavargna-Sani et al. (submitted; left side of the upper Calanca Valley, Zapport Valley, Plattenberg area, and Hennasädel-Heinisch Stafel area). Geologic limits of the newly defined formations are well identified in the new mapped areas; these limits are not newly mapped in other areas. The coordinates represent the kilometric Swiss grid (CH 1903)

distribution of trace elements that are considered as immobile under metamorphic conditions.

Salahorn Formation

The Salahorn Formation is the largest paragneiss formation of the northern Adula basement. The highest peak, Adula (or Rheinwaldhorn, 3,402 m), is composed of these rocks. The type locality is located near the Salahorn peak in the Zapport valley (Fig. 2), where this formation is completely exposed. The Salahorn Formation is principally composed of metamorphosed clastic sediments (Fig. 3b) varying from quartzitic arkose to metapelites. The transitional contacts between these different clastic rocks are clear in the field, leading to the conclusion that they have to be included in the same formation. The Salahorn Formation is rich in carbonates. Carbonates are generally present as centimetric lenses (Fig. 3b) of brown calcitic, ankeritic, or dolomitic marble. Metric lenses of these carbonates can be found locally (Fig. 3c). The Palaeozoic carbonates of the Salahorn Formation are not to be confused with the abundant boudins of Mesozoic sediments folded into the Adula basement. In the Salahorn Formation, there is a close association of metaigneous greenstone and gneiss with the felsic paragneisses. The metaigneous bodies are observable as decimetric to decametric lenses or boudins. Contacts with the clastic country rocks are generally sharp. A transitional contact is sometimes observed.

The appearance and mineralogy of the metaigneous rocks of the Salahorn Formation are quite variable. They can be divided into two types: (a) mafic rocks varying from prasinites to eclogites and (b) amphibole plagioclase gneiss. The mafic rocks of type (a) are very common. They generally have a fine-grained texture, often with symplectites, and they are dark green in colour. Amphibole plagioclase gneiss of type (b) is less mafic and crops out only locally. The texture is medium-to coarse-grained, dominated by hornblende and plagioclases. Two samples were dated at 517–518 Ma ("Salahorn Formation" section). Magmatic contacts are observed between types (a) and (b) (Fig. 3a). Their relative ages seem to be identical based on field relationships. The Salahorn Formation also encloses large ultramafic bodies. The two largest bodies are reported on the map (Fig. 2), one

Fig. 3 Lithologies of the Salahorn Formation. **a** Magmatic rocks of the Salahorn Formation, magmatic contact between the amphibole–plagioclase gneiss and the *dark* mafic rock. Zapport Valley (724340/151890). **b** Albitic meta-arkose containing abundant carbonates in the matrix. Zapport Valley. **c** Carbonates in the micaschists. Zapport Valley (724160/151800)

located at Monte Amianto (720200/153000) and the other located at Cima di Sgiu (718000/153500). The Cima di Sgiu rocks are serpentinites and rodingites, which were described by Deutsch (1979). These bodies are in close association with mafic rocks.

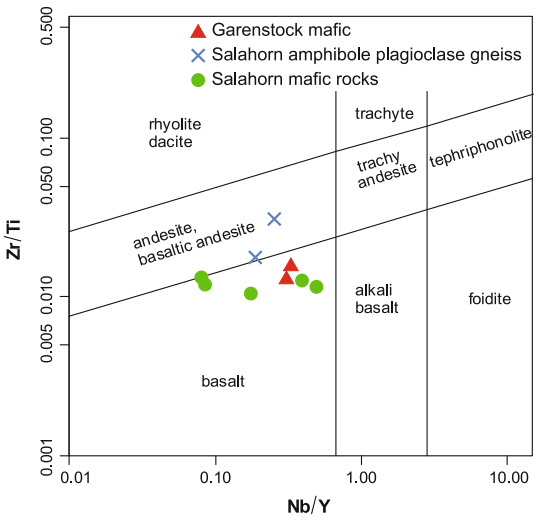

Fig. 4 **a** Mafic magmatic rocks of the northern Adula nappe plotted in the classification diagram of volcanic rocks (Pearce 1996, modified from Winchester and Floyd 1977)

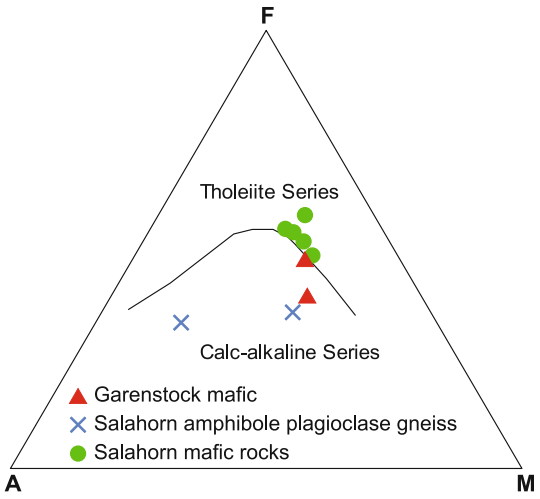

Fig. 5 AFM discrimination diagram of the mafic rocks of the northern (after Irvine and Bargar 1971)

The Salahorn Formation includes partly what was mapped as "Paragneise und Glimmerschifer" by Jenny and Frischkecht (in Jenny et al. 1923) and "Glimmerschifer und Paragneise" by Egli (1966).

The whole-rock chemical composition of the magmatic rock types of the Salahorn Formation was analysed (Online Resource 1). Mafic rocks (a) varying from prasinites to eclogites were interpreted as volcanic rocks based on their texture and the relationships with the nearby paragneiss. Amphibole plagioclase gneiss (b) was interpreted as plutonic. To facilitate comparison of the rocks, both rock types were plotted in classification diagrams of volcanic rocks. Mafic rocks (a) are attributed to basalt (Fig. 4) in the classification of Pearce (1996; modified after Winchester and Floyd 1977). The five samples analysed (Online Resource 1) display a rather large compositional spread from 47 to 53 wt% SiO_2, which does not correlate with the corresponding mg# (63–72), in contrast to what would be expected for a differentiation series. This discrepancy is interpreted as resulting from the contamination of magmas by country rock at the time of emplacement and/or by metamorphic remobilisation. The relatively high Fe_2O_3 contents (12–16 wt%) and low mg# point to some degree of differentiation of these mafic magmas. They lie in the range of tholeiitic basalts in classification diagrams (Fig. 5). The REE-normalised patterns (Fig. 6a) of the five samples also display a large range of LREE values, with La_N ranging from 30 to 100. Nevertheless, three samples display a coherent set of weakly fractionated REE patterns with $La/Lu_N = \sim 1.6$, whereas the two other samples are more enriched in LREE. The absence of an Eu anomaly suggests that no significant plagioclase fractionation occurred during differentiation. The three coherent samples point to a typical pattern of tholeiitic basalts. They also show significant negative anomalies in Ta, Nb, and, to a lesser extent, Ti, coupled with a positive anomaly in Pb in the spider diagrams (Fig. 6b). This distribution of incompatible elements is usually indicative of subduction-related magmas. These anomalies are not expressed at all in the two samples enriched in LREE. Considering the rather large variability and the limited number of analyses, it is not possible to provide an unequivocal interpretation of the geochemical signature of these mafic rocks. Relying on the least REE-enriched samples, we would consider these mafic rocks to be tholeiitic basalts with a calc-alkaline signature, which may correspond to continental or back-arc tholeiites.

The two analyses of amphibole plagioclase gneisses (Online Resource 1) are quite contrasting in their SiO_2 contents (53 and 64 wt%, mg# (79 and 64) and REE concentrations (e.g. La = 7 and 16 ppm, respectively). We attribute this difference to distinct degrees of magma differentiation. Both analyses show striking features, such as very high Sr concentrations (>600 ppm), positive Eu anomalies, and strongly fractionated normalised REE patterns (Fig. 6a; $La/Lu_N = 7–10$) with low HREE contents (spoon-like patterns). Ta and Nb are also very low-generating, strongly negative anomalies in a primitive mantle-normalised diagram (Fig. 6b). The spoon-like REE patterns are typical of differentiated melts from which large amounts of amphibole have been subtracted (Davidson et al. 2007; Alonso-Perez et al. 2009). The positive Eu anomaly coupled with high concentrations of Sr points either to plagioclase accumulation in the rock or to the retarded crystallisation of this mineral in the melt. Altogether, we interpret these chemical characteristics as resulting from the early fractionation of amphibole at relatively high pressures (e.g. at the base of the continental crust) from a hydrated basaltic magma (Alonso-Perez et al. 2009). The high water content

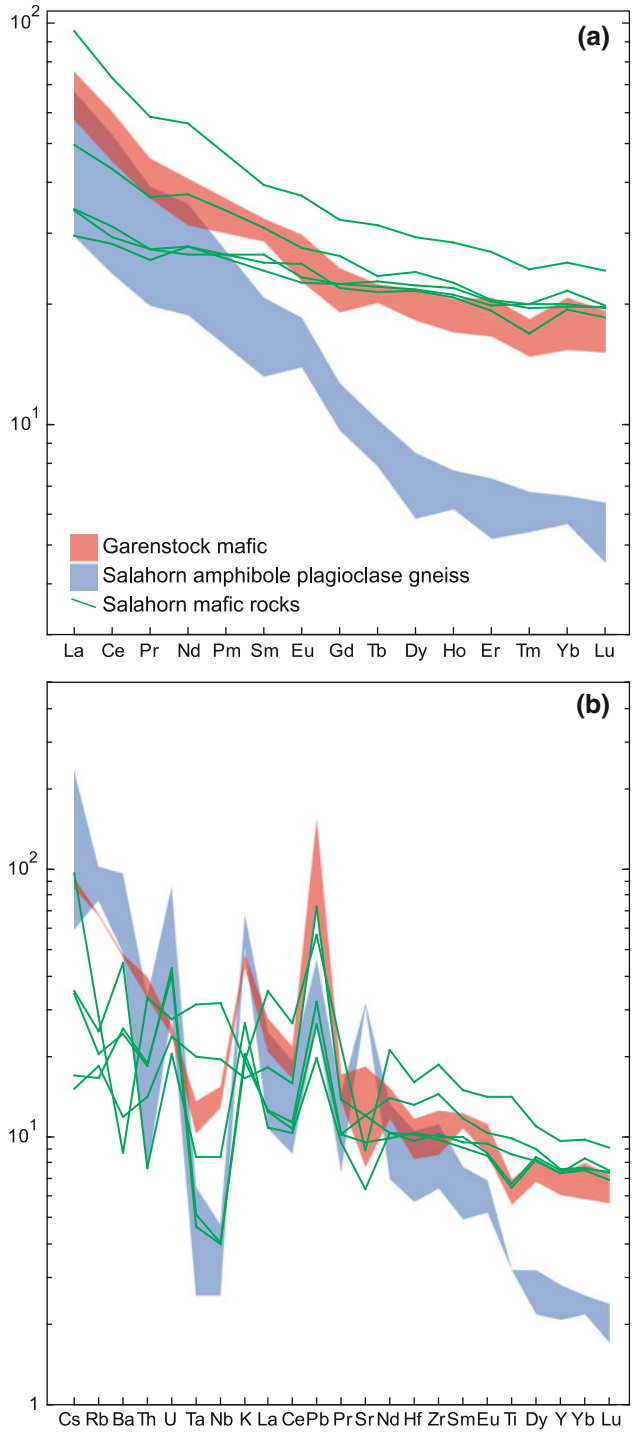

Fig. 6 Variation diagrams of the northern Adula mafic rocks. The areas used for Garenstock mafics and amphibole–plagioclase gneiss represent only two samples. **a** Chondrite-normalised REE diagram (after Sun and McDonough 1989). **b** Primitive mantle-normalised spider diagram (after McDonough and Sun 1995)

and high pressure prevented plagioclase crystallisation, thus enriching the differentiating melt in Sr, Eu, and Al (e.g. Barboni et al. 2011). The formation of the amphibole–plagioclase gneisses would thus require magma differentiation at deep levels in a wet environment in a tectonic context, such as a continental active margin or a back-arc environment (Pearce and Stern 2006).

Given that the Salahorn mafic rocks are tholeiitic with a calc-alkaline signature and are contemporaneous with the amphibole–plagioclase gneisses, we suggest a back-arc geotectonic context for the Salahorn magmatic activity.

Trescolmen Formation

The Trescolmen Formation outcrops in the eastern part of the northern Adula nappe. This formation is composed of metapelites (Fig. 7a) that contain basic boudins. The metapelites are rather homogeneous and show characteristic brown alteration. They are tightly foliated and contain abundant quartz segregations. Phengite and quartz are the dominant minerals. The rock also contains a variable amount of metamorphic minerals, such as garnet, kyanite, staurolite, chloritoid, biotite, paragonite, and albite. The distinctive feature of the rock is the absence of carbonates. The whole-rock chemical composition of the metapelites is rather constant (Cavargna-Sani 2008).

Mafic boudins in the Trescolmen Formation vary from eclogites (Fig. 7b) to prasinites. The contacts between the metapelites and the mafic boudins are always sharp. Spectacular eclogites (Fig. 7b) are preserved in many localities (Hennasädel, Zapport Tal, Alp da Confin, Alp de Trescolmen, Alp de Ganan; see Fig. 2). A few ultramafic boudins are also located in the metapelites of the Trescolmen Formation (Pfeifer et al. 1993).

The geochemical whole-rock composition of the mafic rocks of the Trescolmen Formation was extensively analysed by Santini (1992), yielding the conclusion that the basic rocks have an oceanic origin with a tholeiitic affinity, often with a MORB signature.

Metamorphic conditions recorded by the rocks of the Trescolmen Formation are well studied. The metapelites have suffered a pressure of 25 kbar in the Central Adula Nappe (Meyre et al. 1999; Cavargna-Sani 2008). The metamorphic mineral assemblages in mafic rocks indicate high-pressure peak conditions increasing from north to south (Heinrich 1986; Dale and Holland 2003). The polymetamorphic history of the Trescolmen Formation is well recorded in garnets (Koch 1982; Zulbati 2010; Herwartz et al. 2011). However, only the recent radiogenic ages (Liati et al. 2009; Herwartz et al. 2011) clear the two episodes in these rocks.

Heinisch Stafel Formation

The Heinisch Stafel Formation outcrops in the north-eastern part of the Adula nappe (Fig. 2). This formation is mainly composed of metamorphosed clastic sediments,

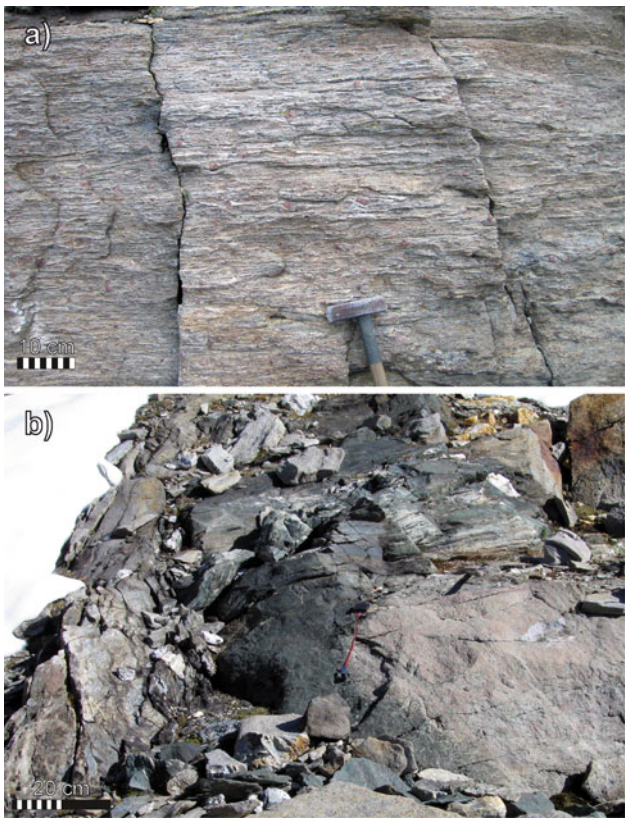

Fig. 7 Lithologies of the Trescolmen Formation. **a** Garnet metapelites. Alp de Ganan (733000/137900). **b** Eclogic mafic boudins with a retrogressed rim in the metapelitic matrix. Alp de Ganan (733100/137780)

which range from micaschists to meta-arkose (Fig. 8b). White mica and chlorite are very abundant; quartz and feldspar occur in more variable amounts. The general colour of this paragneiss is grey to green-grey. In this formation, a clear transition between micaschist and greenstone can be observed (Fig. 8c). This transition is marked by enrichment in chlorite, amphibole, and plagioclase of the micaschist and is very typical and specific to this formation. Considering the traits described above, the protolith of the greenstone layers is interpreted as metatuff. Greenstones can vary from eclogites to prasinites with the presence of layered amphibolites (Fig. 8a), which are dated as Ordovician ("Heinisch Stafel Formation" section). Ankeritic nodules that are smaller than 1 cm are very frequent in this formation, and they occur in both the clastic metasediments and the greenstones.

Garenstock Augengneiss

The Garenstock Augengneiss (Fig. 9a) is an Ordovician ("Garenstock Augengneiss" section) granitoid that is characterised by a prominent augen texture of K-feldspar in a mica-rich matrix occurs in the northern part of the Adula

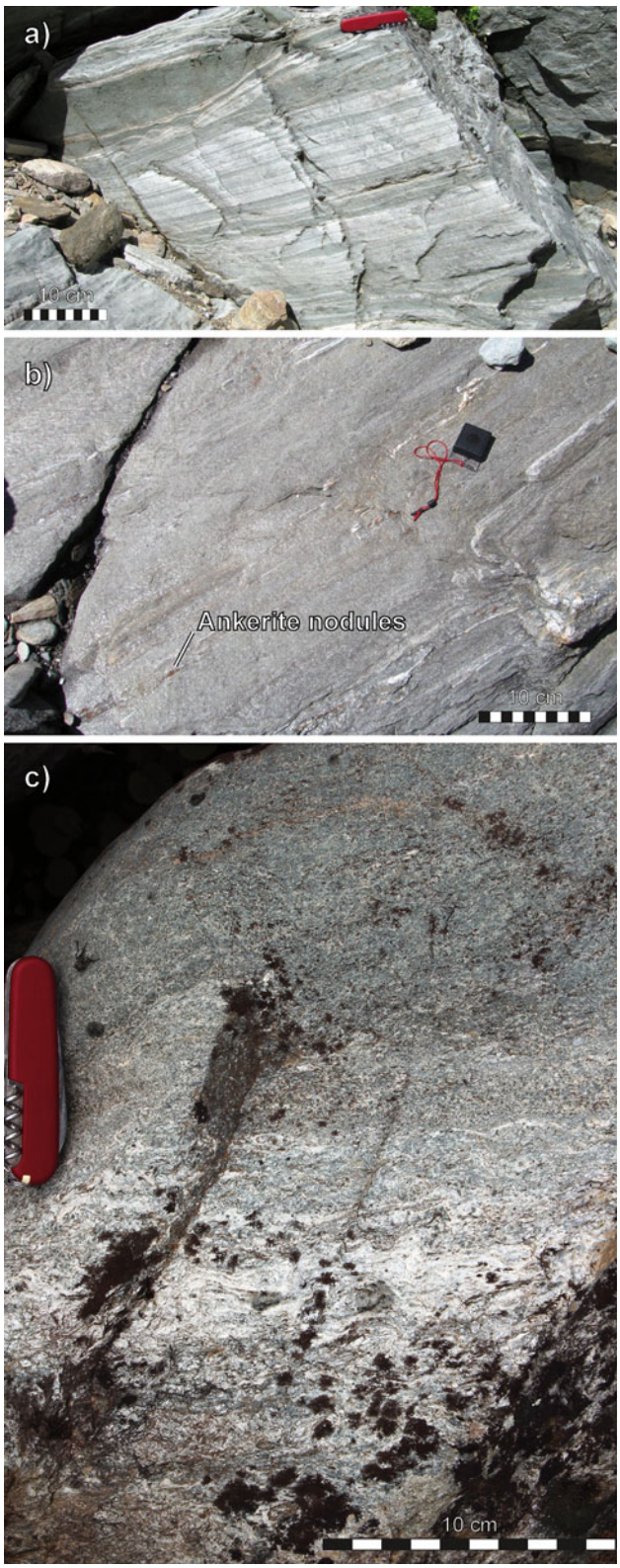

Fig. 8 Lithologies of the Heinisch Stafel Formation. **a** Banded amphibolite, outcrop of sample MC 253. Heinisch Stafel Alp (733500/161800). **b** Micaschist with ankeritic spots. Heinisch Stafel Alp (733500/161800). **c** Transition between micaschist and greenstone, Heinisch Stafel Alp (733500/161800)

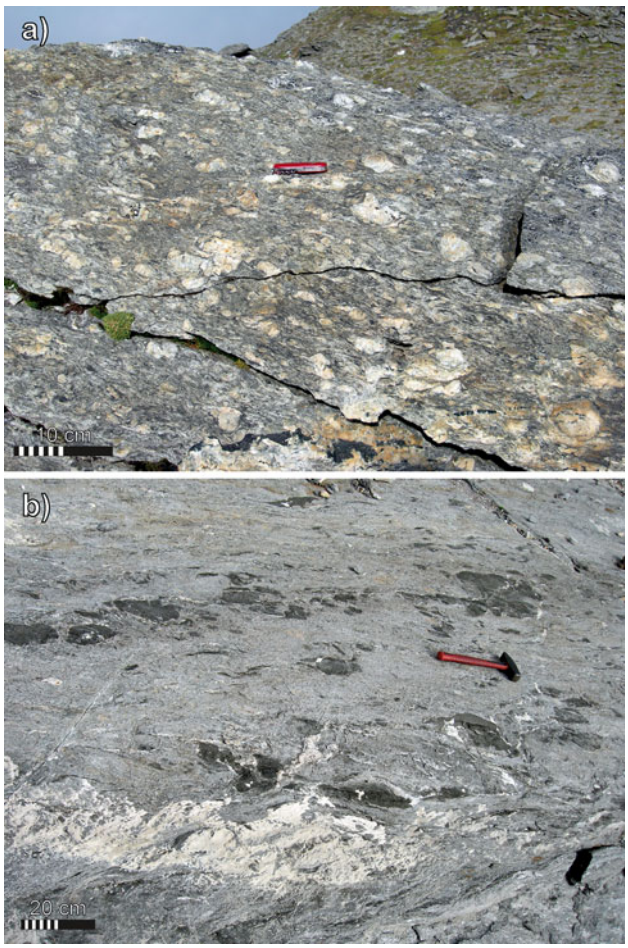

Fig. 9 Ordovician Garenstock Augengneiss of the northern Adula nappe. **a** Granitic augengneiss. Garenstock (721870/157300). **b** Garenstock mafic rock associated with the granite. Garenstock (721870/157300)

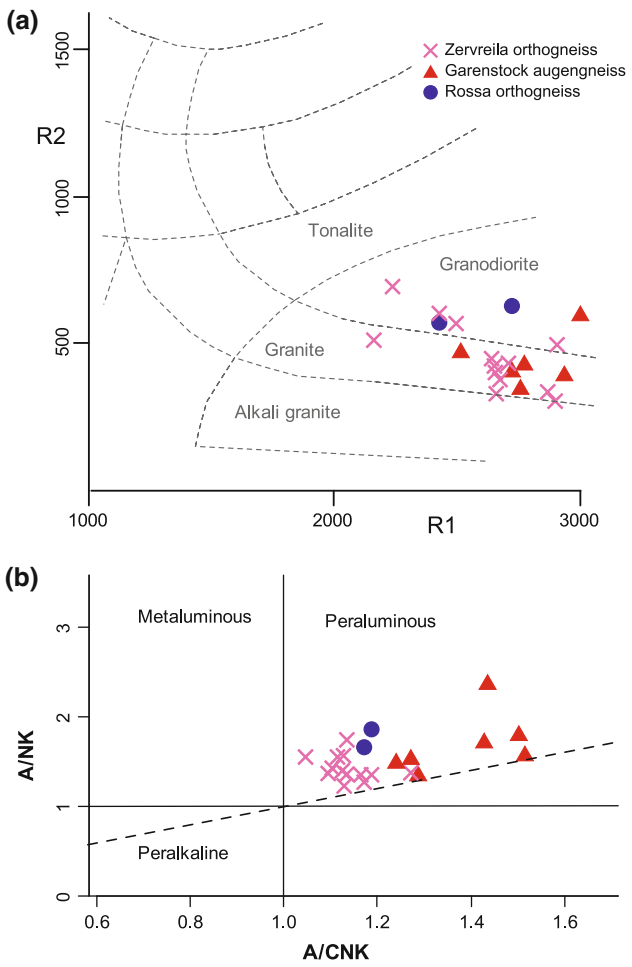

Fig. 10 Classification of the granitoid rocks of the northern Adula. **a** R_1–R_2 diagram (De La Roche et al. 1980); R1 = 4Si − 11(Na + K) − 2(Fe + Ti); R2 = Al + 2Mg + 6Ca. **b** Discrimination diagram for granites derived from Maniar and Piccoli (1989)

nappe. The augen texture is not present everywhere, and a transition to an augen-free gneiss can be observed locally. The gneiss composition is quartz, K-feldspar, plagioclase, white mica, biotite, garnet, epidote, zircon, apatite, and ilmenite. Metric to decimetric mafic boudins and lenses (Garenstock mafic rocks, Fig. 9b) are locally abundant within the augengneiss (Fig. 9b). Eclogite relicts are sometimes present in these boudins. A lithologic description of the Garenstock Augengneiss can be found in Kopp (in Jenny et al. 1923) and Egli (1966).

Garenstock Augengneiss samples (Online Resource 2) are located in the granite field of the R1–R2 classification diagram (Fig. 10a). They are SiO_2 rich (69–77 wt%) and strongly peraluminous (*A*/CNK = 1.2–1.5) (Fig. 10b). Many samples show abnormally low Na2O concentrations below 2 wt% and as low as 0.07 wt% with a K_2O/Na_2O ratio between 1.5 and 3.7 and extreme values above 25. Ba concentrations are high to very high (400–1500 ppm). As mentioned in the introduction, the low-Na samples are interpreted as weathered rocks in relation to a pre-Triassic emersion of the basement (see "Triassic transgression and Mesozoic stratigraphy" section). It is difficult to assess whether all analysed samples have been modified by this alteration event. The zircon morphology is mostly of type S_{13}, S_8, and S_3, which is a distinguishing characteristic of aluminous granitoids (Pupin 1980). In other words, the peraluminous character of the Garenstock granite is partly an original feature of the rock. The REE concentrations (Fig. 11a) are presumably unmodified by alteration processes. Their normalised patterns are consistent with the classic patterns of calc-alkaline granitoids; they show a significant negative Eu anomaly ($Eu/Eu^* = 0.4–0.7$), a fractionated LREE segment ($La/Sm_N = 3.1–3.7$), and a relatively flat HREE ($Gd/Lu_N = 1.2–2.0$). The primitive mantle-normalised spider diagram (Fig. 11b) shows strong negative anomalies in Ta, Nb, Sr, and Ti. Altogether and considering the many contemporaneous mafic lenses hosted by the granite, we tentatively interpret this rock as

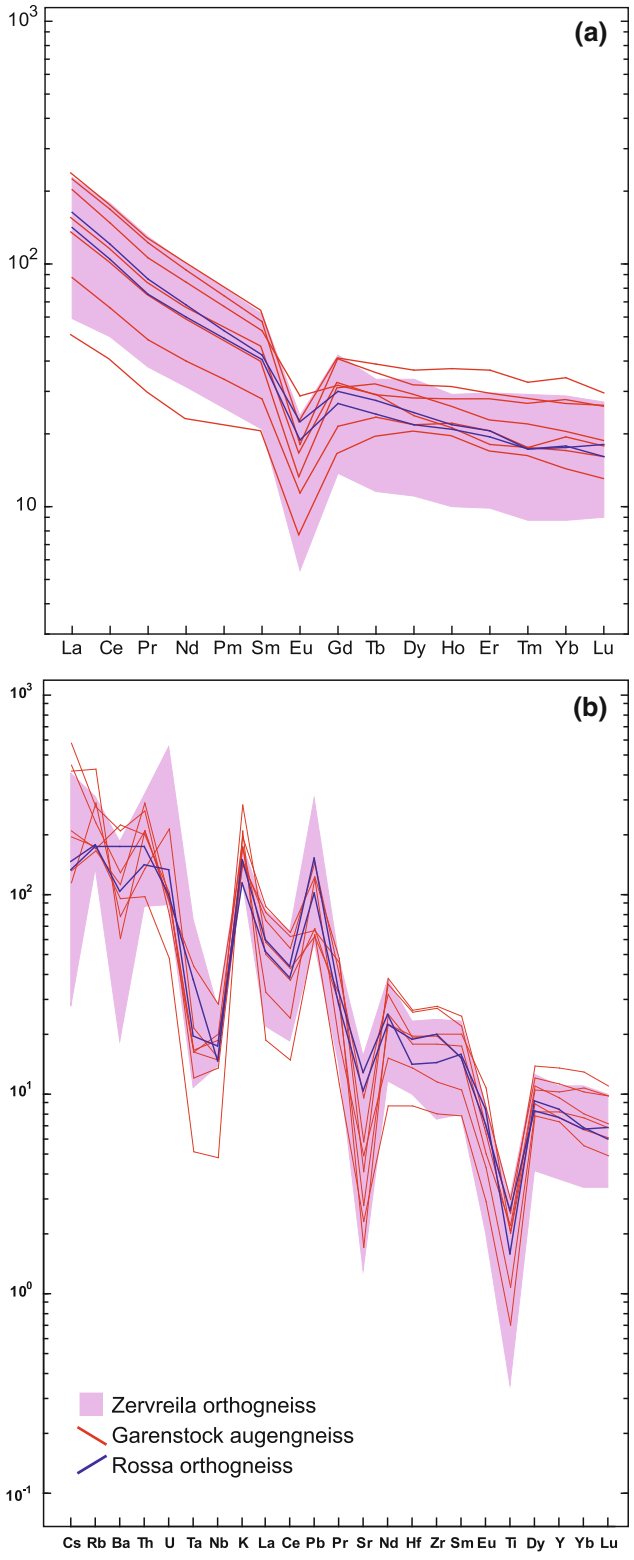

Fig. 11 Variation diagrams of the northern Adula granitoid rocks. **a** Chondrite-normalised REE diagram (derived from Sun and McDonough 1989). **b** Primitive mantle-normalised spider diagram (after McDonough and Sun 1995)

differentiated K-feldspar-rich calc-alkaline granite. Its peraluminous character is most likely a consequence of protracted amphibole fractionation from a wet calc-alkaline melt at deep crustal levels (Alonso-Perez et al. 2009) rather than the result of crustal anatexis, which is also suggested by the lack of inherited zircon cores.

Two samples of Garenstock mafic rocks hosted by the augengneiss were analysed (Online Resource 1). One of them was also dated and yielded an age equivalent to that of the augengneiss (ca. 445 Ma, "Garenstock Augengneiss" section). Garenstock mafic rocks are considered as former microgranular enclaves or dismembered cross-cutting synplutonic dykes of basaltic composition (Fig. 4), and they plot in the calc-alkaline field of the AFM diagram (Fig. 5). Their REE-normalised patterns (Fig. 6a) show a moderately fractionated LREE segment ($La/Sm_N = \sim 2$) and a relatively flat HREE segment ($Gd/Lu_N = \sim 1.3$) without an Eu anomaly. The primitive mantle-normalised spider diagrams (Fig. 6b) exhibit strong negative anomalies for Ta, Nb, and, to a lesser extent, Ti, as well as coupled positive anomalies in K and Pb. All of these geochemical features are characteristic for calc-alkaline basalts related to subduction environments (e.g. Leuthold et al. 2013).

Rossa orthogneiss

The Rossa orthogneiss and the Garenstock Augengneiss are considered separately because they are not connected at an outcrop. They both have the same Ordovician age ("Rossa orthogneiss" section). The Rossa orthogneiss texture is usually fine grained and does not exhibit the characteristic augengneiss texture typical of the Garenstock gneiss. However, some K-feldspar phenocrysts can be locally observed. Mafic boudins are rarely present, and eclogites were not found. Descriptions of this formation can be found in Frischknecht (in Jenny et al. 1923) and Kündig (1926). Frischknecht proposes a distinction between orthogneisses based on biotite content. However, this content in biotite is strongly related to metamorphic grade (Spear 1995) and therefore cannot be used in the formation definition.

The Rossa orthogneiss analyses (Online Resource 2) plot in the fields of granodiorites in the R1–R2 classification diagram (Fig. 10a) and are peraluminous (Fig. 10b) and SiO_2 rich ($\sim$69 wt%). The REE-normalised pattern (Fig. 11a) shows a significant Eu anomaly ($Eu/Eu^* = \sim 0.6$), a fractionated LREE segment ($La/Sm_N = 3.4–3.7$), and a relatively flat HREE ($Gd/Lu_N = 1.5–1.9$). The primitive mantle-normalised spider diagram (Fig. 11b)

shows strong negative anomalies in Ta, Nb, Sr, and Ti. The two Ordovician granites, Garenstock Augengneiss and Rossa orthogneiss, exhibit very similar geochemical characteristics. The small amount of analysed samples does not allow us to compare the magmatic evolution of the two Ordovician granites, but the Rossa orthogneiss seems slightly more depleted in HREE than the Garenstock Augengneiss. Both granites are interpreted as calc-alkaline.

Zervreila orthogneiss

The Early Permian ("Zervreila orthogneiss" section) Zervreila orthogneiss (Fig. 12) is one of the most widespread rock types of the northern part of the Adula nappe. It outcrops at several structural levels (base to top) of the nappe (Fig. 2). The Zervreila orthogneiss is a leucocratic granitic rock, mainly fine grained, sometimes with an augengneiss texture formed by K-feldspar (Fig. 12). The main minerals are quartz, K-feldspar, plagioclase, and phengite. Phengite gives a typical greenish colour to the rock and is the reason why this formation is also classically called "Phengitgneise" (Jenny et al. 1923; Van der Plas 1959; Egli 1966). Biotite becomes more abundant to the south with increasing Barrovian metamorphic conditions. The accessory minerals are epidote, zircon apatite, and garnet. The Zervreila orthogneiss is completely devoid of mafic boudins and other associated rocks. Rare biotite-rich schlieren were most likely enclaves at the origin. Zervreila orthogneiss are Muscovite-bearing peraluminous granitoids according to the classification of Barbarin (1999). A good petrographic description can be found in Jenny et al. (1923) and Egli (1966). The intrusive contacts in the surrounding paragneiss were also described (Egli 1966; Löw 1987). The precise metamorphic conditions recorded by the Zervreila orthogneiss are unknown.

The Zervreila orthogneiss samples (Online Resource 2) plot in the granite and granodiorite fields of the R1–R2 classification diagram (Fig. 10a). They are rich in silica (66–77 wt% SiO_2), peraluminous (Fig. 10b), and alkali-calcic according to the classification of Peacock (1931). The REE-normalised patterns are typical of granitoids (Fig. 11a), with a significant negative Eu anomaly ($Eu/Eu^* = 0.3–0.8$), a fractionated LREE segment ($La/Sm_N = 2.8–4.1$), and a relatively flat HREE segment ($Gd/Lu_N = 0.9–2.2$). The primitive mantle-normalised spider diagram (Fig. 11b) shows strong negative anomalies in Ta, Nb, Sr, and Ti. Zircon morphology is restricted to P-types (Pupin 1980), i.e., the {211} pyramid is absent, a feature typical of "subalkaline" (i.e. alkali-calcic) and alkaline granites according to Pupin (1980). Nevertheless, the Zervreila orthogneiss analyses plot outside the A-type granite field in the discrimination diagrams of Whalen et al. (1987).

Fig. 12 Zervreila orthogneiss. Val Scaradra (719950/157250)

The mineralogical and chemical characteristics of the Zervreila orthogneiss, including zircon morphology, are typical of differentiated K-feldspar-rich alkali-calcic granites, such as the Mont Blanc granite in the western Alps (Bussy et al. 2000). Alkali-calcic granites usually occur in the late stages of orogenic cycles or even during the initiation of subsequent extensional tectonics (Bonin et al. 1998; Barbarin 1999). We suggest that the peraluminous signature of these leucogranites is constrained by crystal fractionation at high pressure (Alonso-Perez et al. 2009) and therefore does not represent simple crustal melts because restitic enclaves are nearly absent and zircon cores are not abundant.

Adula nappe cover

Mesozoic (or younger?) cover rock outcrops in several places in the northern Adula nappe. In most cases, only slices or boudins of dolomitic and calcitic marble can be observed. The thickness of the slices and boudins vary from a few centimetres to several metres. A few outcrops show a more complete autochthonous stratigraphic series (Cavargna-Sani et al. 2010; Galster et al. 2012) that displays a stratigraphic contact with the basement and a characteristic North Penninic Triassic (Galster et al. 2012) sequence at its base. Basement rocks show evidence of surface alteration prior to the Mesozoic sedimentation. Dolocrete and calcrete nodules and lenses (Fig. 13) at the base of the Mesozoic sequence can locally be observed. These formations are equivalent to the well-known pre-Triassic paleosols in less metamorphic domains: Aiguilles rouges (Demathieu and Weidmann 1982); Mont Blanc (Epard 1989); and Aar (Gisler et al. 2007). Clear stratigraphic contacts of the Adula nappe cover are found on the Garenstock Augengneiss, the Salahorn Formation, the Trescolmen Formation, and the Heinisch Stafel Formation. Carboniferous or Permian clastic sediments of Verrucano type were not found on the older basement.

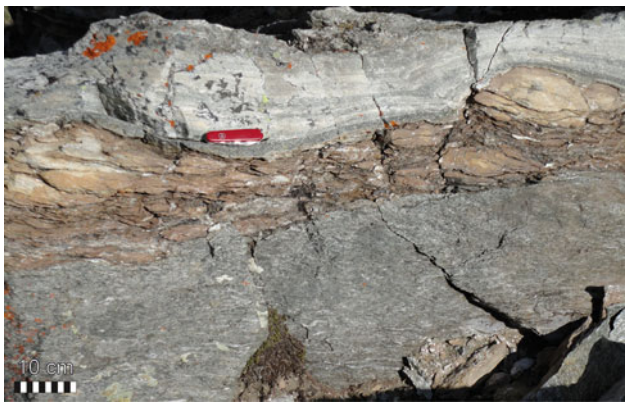

Fig. 13 Dolocrete on the Garenstock Augengneiss and below Triassic quartzite interpreted as pre-Triassic paleosol (see text). Plattenberg area (721600/157250)

Zircon geochronology

Method

Rock samples of several kilograms in mass were crushed and ground to a powder using an oscillatory tungsten carbide disc. Zircons were extracted with manual panning and the use of heavy liquid if necessary. Magnetic separation was used to separate the zircons from magnetic minerals and to select non-metamict zircons. Transparent, "gem"-quality zircons were selected by hand picking. The morphology of the selected zircon grains was studied using secondary electron (SE) imaging with a SEM (Tescan Mira LMU, University of Lausanne).

Zircons used for dating were chemically abraded following a modified procedure described by Mattinson (2005). The zircons were thermally annealed at 800 °C for 10 h and then leached in a mixture of concentrated HF and HNO_3 at 110 °C for 12 h. They were then carefully rinsed with distilled water, mounted in epoxy resin, abraded to the (approximately) equatorial plane, and polished. The textures of each single zircon were investigated through cathodoluminescence (CL) imaging by SEM (CamScan MV2300, University of Lausanne).

The analyses of the zircons were performed using a mono-collector Element XR sector-field instrument interfaced with an UP-193 excimer ablation system (University of Lausanne). The analytical approach applied is outlined by Ulianov et al. (2012). The operation conditions included a 35–25-µm spot size, an on-sample energy density of 2.1–2.3 J/cm^2, and a repetition rate of 5 Hz. A GJ-1 standard zircon (Pb^{206}–U^{238} age of 600.5 ± 0.4 Ma; Schaltegger et al. unpublished) was used as an external standard. The 91500 standard (Wiedenbeck et al. 1995) was measured on each run to monitor the accuracy. The ratio-of-the-mean intensity method was used for the data treatment using LAMTRACE software (Jackson 2008). No correction for common lead was applied because of the presence of mercury in the system and low $(Hg + Pb)^{204}$ intensities. Instead, a qualitative control for the presence of anomalously high $(Hg + Pb)^{204}$ net intensity values was utilised and indicated low-to-negligible common Pb contents. The CL image and the intensity versus ablation time plots were accurately controlled to avoid the analysis of domains potentially enriched in common lead and/or lead losses in each measurement. Only concordant or sub-concordant zircon ages were considered.

Salahorn Formation

Zircons were found in one sample of the metaclastic sediments (MC 353) and in two samples of the magmatic amphibole plagioclase gneiss (MC 209, MC 336). This gneiss corresponds to group (b) of the mafic rocks described in "Salahorn Formation" section. In mafic rocks of group (a), zircons were observed by BSE in thin sections but were very small (<20 µm), usually interstitial, and rich in amphibole inclusions. Their internal texture is homogeneous, and they are most likely of metamorphic origin. No zircon grains were obtained from samples of mafic rocks of type (a).

The paragneiss sample MC 353 is composed mainly of quartz, albite, white mica, and chlorite and contains a few ankerite grains. The sampled outcrop shows a transition to micaceous garnet gneiss. Zircons in this sample have a size of approximately 50–250 µm and are of pale pink colour. Morphologically, these zircons form a homogeneous population. They present a clear crystalline shape with well-developed prisms and pyramids usually found in plutonic rocks (Fig. 14i). Distinct oscillatory zoning is ubiquitous. Xenocrystic cores or metamorphic overgrowths were not found. The analysed zircons form a surprisingly homogeneous age population for a paragneiss (Online Resource 3). Even with the sedimentary origin of the sample, we chose to calculate the median age using the TuffZirc algorithm (Ludwig and Mundil 2002) and did not retain only the youngest age; the age distribution is unimodal, and the possibility of radiogenic lead loss during metamorphism cannot be ruled out. The calculated median age is 518.3 +4.0 −3.5 Ma (Fig. 15b). We interpret that this age is close to the sedimentation age of this formation (see the discussion in Chapt. 4.1).

Zircons in the amphibolite gneiss (MC 209, MC 336) are very abundant. Their sizes range from approximately 30–500 µm, and they are pink coloured. The crystal habit is essentially defined by elongated prisms without pyramids (Fig. 14h). The texture of the amphibolite gneiss zircons is homogeneous or broadly zoned (Fig. 14h). Xenocrystic cores or metamorphic overgrowths were not found. The

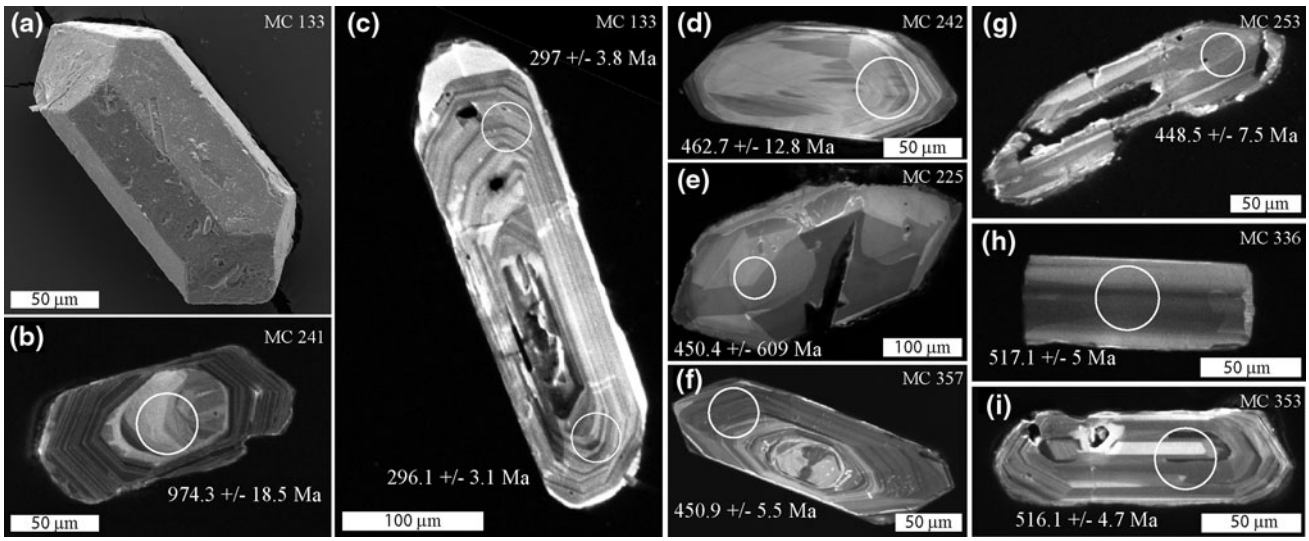

Fig. 14 Selected zircon images from the analysed samples. **a** Zervreila orthogneiss zircon, secondary electron (SE) image (Tescan Mira LMU, University of Lausanne). **b–i** Cathodoluminescence (CL) images of polished zircon sections (CamScan MV2300, University of Lausanne). *Circles* represent the LA-ICPMS analysis according to the respective $^{206}Pb/^{238}U$ age. All indicated ages are concordant. The sample numbers are indicated on each zircon

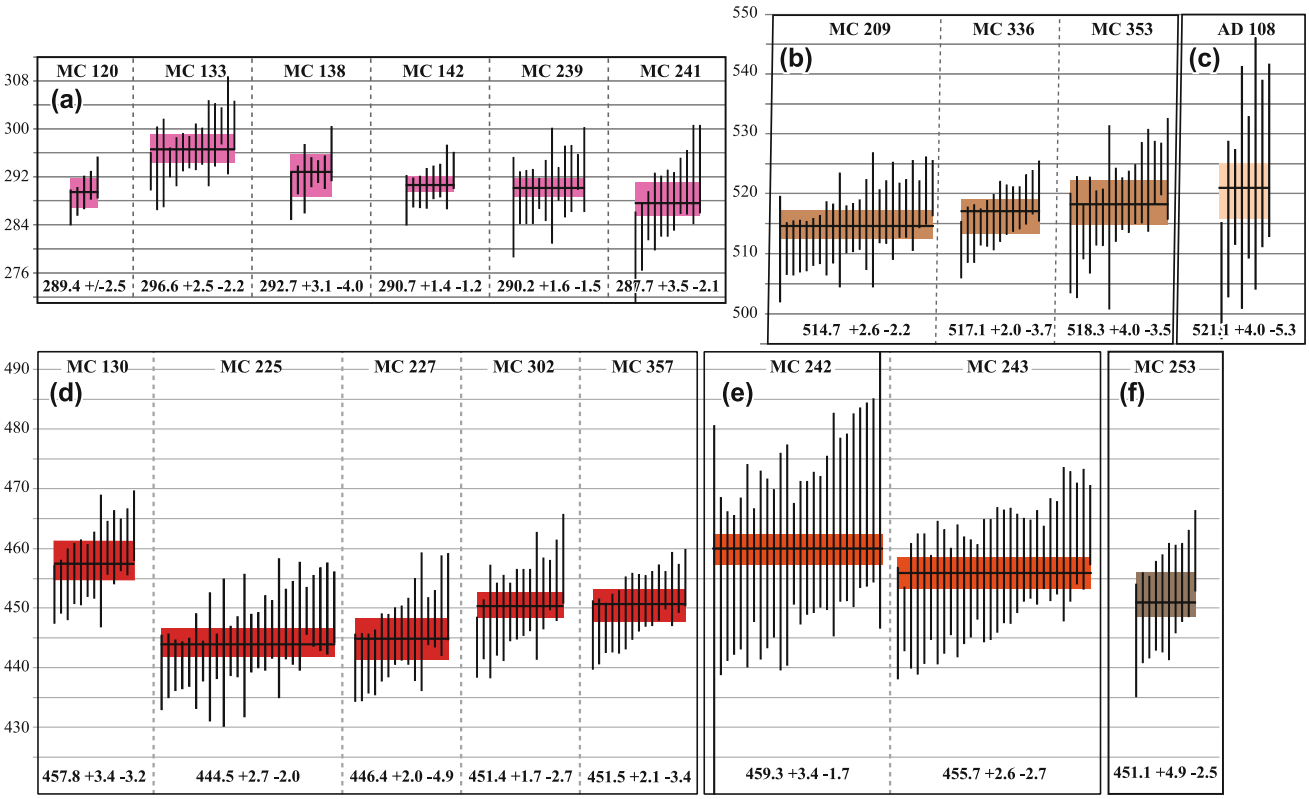

Fig. 15 Calculated $^{206}Pb/^{238}U$ age of each sample. The age calculations were performed using Isoplot (Ludwig 2003) and the TuffZirc equation (Ludwig and Mundil 2002) based on the $^{206}Pb/^{238}U$ age. The median of the largest cluster is taken as the true age, with 95 % confidence errors. The uncertainty of each measurement is given as 2σ. Only concordant or sub-concordant analytical points were used. The same scale was used for all samples. **a** Zervreila orthogneiss. **b** Salahorn Formation: one amphibole plagioclase gneiss and one paragneiss (MC 353). **c** Trescolmen Formation mafic boudin (zircon extracted by Lucia Santini). **d** Garenstock Augengneiss metagranites and one mafic rock (MC 225). **e** Rossa orthogneiss. **f** Heinisch Stafel Formation metatuff layer

calculated median TuffZirc ages (Online Resource 3) of these two samples are similar at 514.7 +2.6 −2.2 and 517.1 +2.0 −3.7 Ma (Fig. 15b). These ages are interpreted as a magmatic age because of the lack of metamorphic overgrowths and the oscillatory zoning of the analysed domains.

Trescolmen Formation

A few zircons of a kyanite eclogite (AD 108; extracted by Lucia Santini) were analysed. Five multigrain zircon fractions were previously analysed by Santini (1992) using ID-TIMS. Concordant or nearly concordant ages ranging between 520 and 540 Ma were obtained by this author.

The zircons analysed in our study are small, elongated grains with a broad oscillatory zoning. The measured age (Online Resource 3; Fig. 15c) is 521.1 +4.0 −5.3 Ma. This age is interpreted as magmatic and confirms the previous results obtained by Santini (1992).

Garenstock Augengneiss

Four samples of the Garenstock Augengneiss (MC 130, MC 227, MC 302, and MC 357) and one sample of an amphibolite boudin (MC 225) were analysed. The Garenstock Augengneiss is very rich in zircon. Their size ranges between 50 and 500 μm, and their colour is generally white, grey, or colourless. The crystal edges are generally slightly smoothed, but the crystalline form is still well identifiable. Textures of the zircon show good magmatic oscillatory zoning (Fig. 14f) with a locally thin (<5 μm) metamorphic overgrowth. A few xenocrystic cores were observed and analysed. The CL images of several zircons show some patches, most likely indicating late lead losses. The calculated median ages of the four Garenstock Augengneiss samples are 457.8 +3.4 −3.2, 446.4 +2.0 −4.9, 451.4 +1.7 −2.7, and 451.5 +2.1 −3.4 (Online Resource 3; Fig. 15d). The magmatic origin of these ages is supported by the CL features of the analysed domains and by the reproducibility of the age. The xenocrystic cores yielded ages of 518.9 ± 6.1, 572.1 ± 5.9, and 579.4 ± 7.3 Ma (Online Resource 3). It was not possible to analyse the metamorphic rim.

The amphibolite sample (MC 225) provided a reasonable amount of zircon with variable morphology and texture. Many crystals are lacking the pyramids, presenting only prisms; some grains with pyramids are similar to the zircons of the augengneiss but slightly rounded (Fig. 14e). Only a few grains show a clear oscillatory zoning. More frequently, the zircons are unzoned or present a broadly patchy zoning (Fig. 14e). Xenocrystic cores are relatively abundant. The ages of the analysed zircons were coherently distributed (Online Resource 3; Fig. 15d), and the median calculated age was 444.5 +2.7 −2.0 Ma. This age is interpreted as magmatic due to the coherency of the analysed spot and the reproducibility of the data. Xenocrystic cores have ages of 540.9 ± 5.7, 555.2 ± 5.4, and 901.9 ± 7.6 Ma.

The age obtained from the amphibolite is identical, within the uncertainties, to the orthogneiss ages, which suggests a contemporaneous emplacement of both magmatic rocks that is also confirmed by the narrow association of these two magmatic rocks in the field.

Rossa orthogneiss

Two samples (MC 242 and MC 243) were analysed. The size of the extracted zircons ranges from 50 to 300 μm, and the zircons are white, grey, or pale pink. The morphology of the Rossa orthogneiss and the Garenstock Augengneiss zircons is almost identical. They are categorised as S-type according to the Pupin (1980) classification. The zircons are oscillatory zoned (Fig. 14d) locally with a thin (<5 μm) overgrowth. A few xenocrystic cores were found. The two samples yielded nearly equal calculated ages of 459.3 +3.4 −1.7 and 455.7 +2.6 −2.7 Ma (Online Resource 3; Fig. 15e), which are interpreted as magmatic ages. One concordant xenocryst age was 533 ± 10.8 Ma.

Heinisch Stafel Formation

Zircons were found in one sample of banded amphibolite (Fig. 8a, MC 253). These zircons are relatively small (30–150 μm) and mainly prismatic and usually have a central channel. They are often xenomorphic. The CL texture is generally homogenous or exhibits a broad patchy zoning (Fig. 14g). A few grains show oscillatory zoning. The calculated median age is 451.1 +4.9 −2.5 Ma (Online Resource 3; Fig. 15f), interpreted as the magmatic age of the volcanic rocks.

Zervreila orthogneiss

The Zervreila orthogneiss is rich in zircons. Their size ranges from 50 to 300 μm, and they are colourless to pale pink in colour and generally idiomorphic (Fig. 14a). They do not show any traces of abrasion, resorption, or overgrowth. Morphologically, the Zervreila orthogneiss zircons are mainly P-type zircons (Fig. 14a) according to the Pupin (1980) classification. The CL texture of Zervreila orthogneiss zircons usually shows a magmatic narrow oscillatory zoning (Fig. 14b, c). Some xenocrystic cores are present but not frequent (Fig. 14c). Zircons affected by metamictisation are very common in the Zervreila orthogneiss. The elevated uranium content in these zircons is reflected by high U intensities in LA-ICPMS spectra.

Six samples of Zervreila orthogneiss (MC 120, MC 133, MC 138, MC 142, MC 239, and MC 241) were analysed. They were distributed throughout the northern Adula nappe (sample location on Fig. 2). The median TuffZirc ages for the six samples are as follows: 289.4 ± 2.5, 296.6 +2.5 −2.2, 292.7 +3.1 −4.0, 290.7 +1.4 −1.2, 290.2 +1.6 −1.5, and 287.7 +3.5 −2.1 Ma (Online Resource 3; Fig. 15a). The CL textures and the age reproducibility clearly point to a magmatic age interpretation. Xenocrystic cores in all samples yielded concordant ages of 423.1 ± 6.4, 451.9 ± 6.8, 521.4 ± 14, and 974.3 ± 18.5 Ma (Online Resource 3).

Discussion

Cambrian sedimentation and magmatism

Two magmatic rocks of the Salahorn Formation (amphibole–plagioclase gneiss) were calculated to have ages of 514.7 +2.6 −2.2 and 517.1 +2.0 −3.7 Ma. The Salahorn Formation Mafics (magmatic rocks of type a) could not be dated, but their ages are interpreted as being approximately the same as that of the amphibole–plagioclase gneiss intrusion based on field relations. Mafic rocks (type a) are widespread and are interpreted as volcanic deposits that are tholeiitic in nature with a calc-alkaline signature. Amphibole–plagioclase gneiss (type b) is less common and has a continental active margin or a back-arc environment geochemical signature. Both magmatic rocks are consistent with a back-arc geotectonic context. A very similar rock association (but Ordovician in age) was interpreted as a result of a continental break-up unrelated to contemporaneous subduction by Pin and Marini (1993). Nevertheless, an interpretation based only on the geochemistry of the geotectonic setting of the emplacement of these magmas is questionable. The interpretation of their emplacement also has to consider the sedimentary context of the surrounding metasediments.

The protolith of the Salahorn Formation paragneiss is a clastic sediment composed of felsic non-mature detrital material and a considerable amount of carbonates. The source rock is quartzofeldspathic with some carbonates. This detrital sedimentation can be related to high-energy epicontinental sedimentation. Zircons from a paragneiss of the same formation yielded an age of 518 +4.0 −3.5 Ma (Table 1). The detrital zircons contained in the clastic metasediments have nearly the same age as the magmatic bodies intruding upon these sediments. The homogeneous age of detrital zircons, its similar age with the magmatic ones, and the immature character of the sediments points to a proximal deposition and to a short time period between erosion and emplacement of the source.

We compare the Salahorn Formation with situation described in the southern Peruvian magmatic arc, where Jurassic magmatic rocks intrude a clastic formation containing detritic zircons less than 3 Ma younger than the intrusion (Boekhout et al. 2012). Boekhout et al. (2012)

Table 1 Sedimentation and magmatic ages of the northern Adula nappe basement formations. Alpine basement events were obtained from von Raumer et al. (2013)

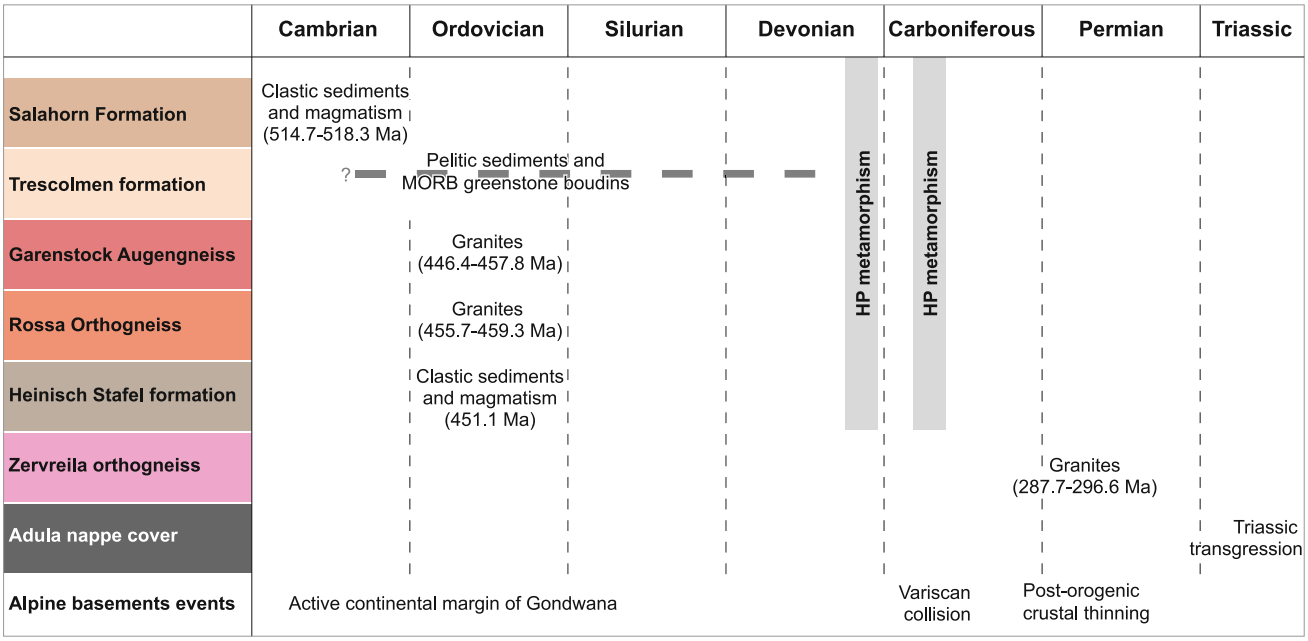

demonstrated the rapid subsidence of the arc slope (with clastic sedimentation) in which arc-related magma intrudes.

The carbonates are most likely also of detrital origin because continuous carbonate beds were never found. A correspondence for the source can be found in the carbonate platforms documented in the Early Middle Cambrian time on the Gondwana margin (Cocozza 1979; Liñán et al. 1993; Elicki 2006).

Large ultramafic bodies are also observed in the Salahorn Formation. In the Alpine basements, ultramafic–mafic bodies are classically interpreted as remnants of oceanic crust and Palaeozoic ophiolite series (Pfeifer et al. 1993). The occurrence of these ultramafic bodies proves the presence of an oceanic domain or a continental breakup process, concomitant to the Salahorn Formation deposit and magmatism. The mechanism by which to integrate these bodies in the clastic sediments can only be hypothetical; however, we suggest that mantle exhumation during rifting processes (Froitzheim and Manatschal 1996) is involved. Variscan and Alpine deformations are certainly responsible for the present-day geometry of the bodies enclosed within the basement.

Eclogites were found in the mafic rocks of the Salahorn Formation, but their age is unknown. Palaeozoic eclogitisation, in addition to the Alpine eclogitisation, can perhaps be considered equivalent to that of the Trescolmen Formation. Zircons from this formation do not retain clear metamorphic rims.

Several correspondences can be mentioned for a correlation of the Cambrian Salahorn Formation. An association of ultramafic and mafic rocks is also found at Loderio (near Biasca, Ticino) in the Lower Penninic under the Simano nappe. These rocks are also dated at 518 ± 11 Ma (U–Pb on zircon), and the mafic rocks show a MORB signature (Schaltegger et al. 2002). Cambrian magmatic rocks (528 ± 6 Ma) are also documented from the Cima di Gagnone area (Gebauer 1995) in the Cima Lunga Nappe. Bussien et al. (2011) noted a 540 Ma age for a banded mafic complex in the Sambuco-Maggia nappe. Cambrian clastic sediments, including intrusive and volcanic magmatic rocks, are noted in the External Crystalline Massifs (Guillot and Ménot 2009). Carbonates in the Early Palaeozoic Paragneisses are documented in these massifs as well (von Raumer and Bussy 2004). Signs of extensive normal faulting and of strong subsidence are widespread in the Early Middle Cambrian (Elicki 2006) and indicate a rifting process. Von Raumer et al. (2013) interpreted the Cambrian paleogeography of the Alpine basement rocks along the Gondwana margin involving an active margin followed by a complex pattern of back-arc rift opening.

Trescolmen Formation: age and emplacement

The Trescolmen Formation has the largest amount of geochronological data in the entire Adula nappe. However, the sedimentation age of this metapelitic formation and the age of the abundant mafic rock emplacement are difficult to determine. A kyanite–eclogite sample (AD 108) yielded an age of 521.1 +4.0 −5.3 Ma (Fig. 15c), the same age as that of the Salahorn Formation magmatism ("Cambrian sedimentation and magmatism" section). Other zircon protolith ages were obtained for the mafic rocks of the Trescolmen Formation, such as 461 +4 −5 Ma (Santini 1992, concordant TIMS age). SHRIMP ages determined by Liati et al. (2009), sometimes obtained from a small number of analyses, are 587 ± 5 Ma (Pl Qtz Grt WM Am gneiss, sample CON 6), 595 ± 9 Ma (eclogite, sample CON 7), 561 ± 22 Ma (eclogite, sample TRE 5, based on 2 analyses), 655 ± 12 Ma (eclogite, sample TRE 6, based on one analysis), and 482 ± 8 Ma (eclogite, sample TRE 8, based on two analyses). The youngest magmatic core in zircons from the metapelites, interpreted as a minimum sedimentation age, is dated at approximately 460 Ma (Liati et al. 2009). The magmatic rocks included in the metapelites are all older than this minimal sedimentation age, except one sample of the same Ordovician age. The Palaeozoic HP metamorphic age is better constrained at ca. 370 and 340 Ma (Liati et al. 2009; Herwartz et al. 2011).

The metapelites protolith is likely a fine-grained, mature, carbonate-free, clastic sediment that can be categorised as shale. The bulk rock chemical composition of the lithology is in agreement with this interpretation (Cavargna-Sani 2008), and the sedimentation was most likely marine. The mafic boudins are mainly characterised as basalts due to their fine texture. The basic rocks of the Trescolmen Formation have a MORB signature (Santini 1992) and are interpreted to be of oceanic origin. The nature of the contact between the mafic boudins and the metapelitic matrix in the Trescolmen Formation cannot be clearly determined: they always appear sharp in the field. The protolith ages of the mafic boudins are older than the youngest detrital zircon in the metapelitic matrix. This lithological association, and the scattered ages of the magmatic rocks, is typical for a detrital formation with blocs of older igneous rocks (Wildflysch-type deposit), or for a tectonic melange. Both interpretations imply that the Trescolmen Formation could represent a highly deformed zone, typical of a terrane accretion (also proposed by Liati et al. 2009) or an accretionary prism related to subduction.

The formation age of the Trescolmen Formation protolith is very difficult to determine accurately. The maximum age is constrained by the youngest detrital zircon in the metapelitic matrix (~460 Ma; Liati et al. 2009). The

minimum age is given by the age of the oldest high-pressure event at ~370 Ma (Table 1; Liati et al. 2009). The age and the emplacement of the protolith most likely correspond to a mélange formed during the subduction, producing the Variscan orogeny.

Analogies of the Trescolmen Formation can most likely be found in the Lac Cornu area in the Aiguilles Rouges Massif (Liégeois and Duchesne 1981; von Raumer and Bussy 2004). In this area, mafic eclogites are included in various metasedimentary clastic rocks. Their age corresponds to the period between 463 Ma (Bussy et al. 2011; the basaltic protolith) and 321 Ma (Bussy et al. 2000; a high-temperature event that post-dates the high-pressure events). The paleogeographic context of the Trescolmen Formation protolith emplacement and the high-pressure metamorphism must be assigned to the Variscan orogeny. This interpretation is consistent with the general evolution of the Pre-Mesozoic Alpine basements (von Raumer et al. 2013).

Ordovician evolution

Two analysed samples of the Rossa orthogneiss yielded ages of 459.3 +3.4 −1.7 and 455.7 +2.6 −2.7 Ma (Fig. 15e); these two ages overlap within errors. Four ages of metagranites of the Garenstock Augengneiss are between 446.4 and 457.8 Ma (Fig. 15d; Table 1), and one amphibolite sample (interpreted as a metagabbro) from a boudin included in the metagranite has an age of 444.5 +2.7 −2.0 Ma (Fig. 15d, MC 225). Although these values overlap only partially within the errors, we assume that they are the expression of the same Ordovician magmatic episode. Field criteria suggest interpreting the Rossa and Garenstock granites and the associated mafic rocks as K-rich calc-alkaline granitoids within the Barbarin (1999) granite classification. Geochemical characteristics suggest interpreting the granites as K-feldspar-rich calc-alkaline granites and a concomitant calc-alkaline basaltic magma. They are emplaced in an active margin geodynamic environment.

Ordovician granitoids are common in the Alpine basements. In the Lower Penninic nappes, Ordovician granitoids were identified in the Sambuco-Maggia nappe (Bussien et al. 2011) and in the Monte Leone nappe (Bergomi et al. 2007). In the better known External Massifs, they are found in the Gotthard and Tavetsch Massifs (Oberli et al. 1994), the Aar Massif (Schaltegger et al. 2003), and the Aiguilles Rouges and Mont Blanc Massifs (von Raumer and Bussy 2004; Bussy et al. 2011). For a more complete dataset, the reader is referred to the reviews by Schaltegger and Gebauer (1999), von Raumer et al. (2002), and Schulz et al. (2008).

The Heinisch Stafel Formation can be interpreted as a typical volcano–sedimentary basin deposit. One sample in the volcanic interlayer yielded zircons of 451.1 +4.9 −2.5 Ma (Fig. 15f). This age is interpreted as the deposition age of the volcano–sedimentary series. Further volcano–sedimentary basins of this age are documented in the Alpine realm. Gansser and Pantic (1988) studied the metamorphosed volcanic–sedimentary series of the Edolo Schists (Southern Alps, bordering the Tonale Line) and dated it by palynomorphs. In the Middle Penninic Métailler nappe, volcanic–sedimentary deposits are also dated at ca. 460 Ma (Gauthiez et al. 2012). The Heinisch Stafel volcano–sedimentary formation is almost contemporaneous with the emplacement of the Ordovician Rossa and Garenstock granites.

The reviews by Stampfli et al. (2011) and von Raumer et al. (2013) suggest a subduction zone under the N-Gondwana continental margin (the future Alpine basements). This subduction zone involves the production of large amounts of Ordovician magmatic rocks. These reviews suggest a crustal extension for the pre-Alpine basements from the Middle Ordovician. This scenario can also be assumed for the emplacement of the formations described above.

Variscan metamorphism

The Variscan orogeny in the Adula nappe is evidenced by a few Variscan metamorphic ages. Liati et al. (2009) describe two generations of metamorphic rims in zircons (370 and 330–340 Ma) both interpreted as high-pressure events based on REE patterns. Herwartz et al. (2011) report a minimum Lu–Hf garnet age of ~330 Ma. This age is not related to specific metamorphic conditions. Traces of granulitic metamorphism or migmatisation were never observed.

The 370 Ma, probably high-pressure, metamorphic event can be ascribed to the Devonian subduction phase (early Variscan; Stampfli et al. 2002; von Raumer et al. 2009, 2013; Guillot and Ménot 2009). The eclogite facies rocks of the Lac Cornu area in the Aiguilles Rouges Massif have a possible age close to 345 Ma (Bussy et al. 2011). The successive high-temperature decompression melting after the eclogite facies is better constrained and dated at ~320 Ma in the Aiguilles Rouges Massif (Bussy et al. 2000).

The contact between the previously described formations (Salahorn Formation, Trescolmen Formation, Heinisch Stafel Formation, and the Garenstock and Rossa orthogneisses) is perhaps a result of the Variscan nappe stack. This nappe stack is proven in less deformed Alpine Palaeozoic terrain (Guillot and Ménot 2009).

Late Variscan granites and tectonic

The six studied Zervreila orthogneiss samples were found to have ages between 287.7 and 296.6 Ma (Fig. 15a; Table 1). Six ages overlap within errors. MC 133 is the oldest and overlaps only partially with the other samples. However, field criteria or geochemistry do not show evidence for a clearly different magmatic event. We therefore interpret the whole Zervreila orthogneiss as having been formed during a single magmatic event, but most likely composed of different intrusion pulses at approximately 292 Ma. The mineralogical and geochemical characteristics of the Zervreila orthogneiss suggest a tardi- or post-orogenic geotectonic environment for their emplacement. Well-preserved magmatic contacts between the Zervreila orthogneiss and the other formations have not been observed. The present geometry (Fig. 2) suggests that the Zervreila granite intruded the older polymetamorphic formations, forming a structured Variscan basement at this time (Fig. 16).

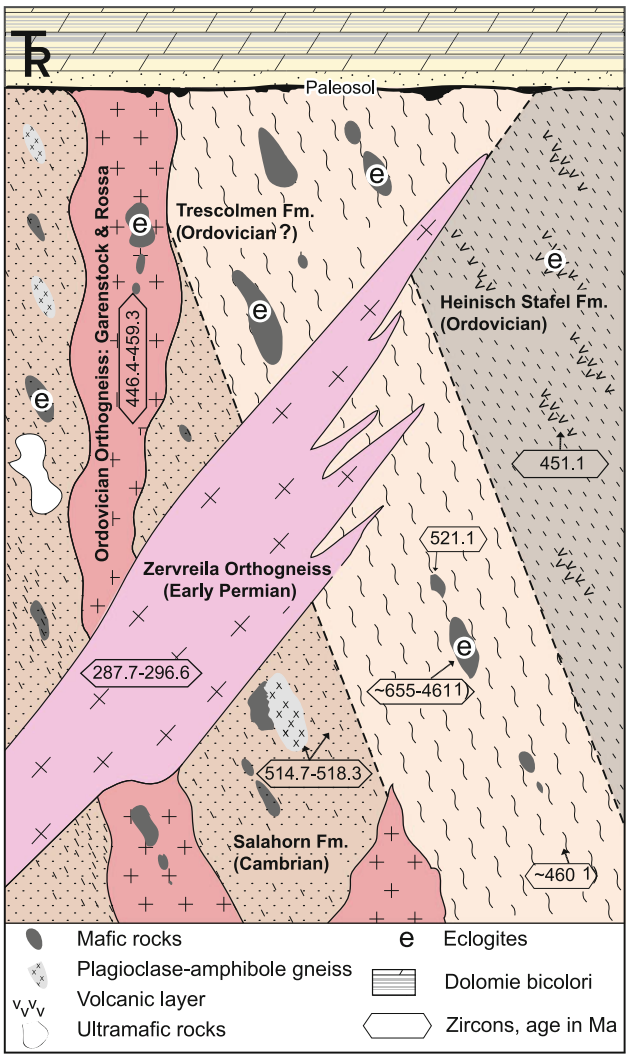

Fig. 16 Adula nappe basement formations and age relations. Ages indicated with 1) are based on the work of Liati et al. (2009)

Molasse-type detrital sediments of Late Palaeozoic–Early Triassic (Verrucano) are not found in the Adula nappe. Alterations and paleosols under the Triassic sedimentary cover are clearly revealed on the Garenstock Augengneiss of the Plattenberg area, which suggests that the northern Adula nappe basement was exposed prior the Triassic transgression and most likely formed a topographic high during the Permian basin-and-range tectonic environment. The Adula history contrasts with that of the nappes placed north of it in the Triassic paleogeographic environment (Luzzone-Terri nappe, Lucomagno nappe, and Gotthard nappe) because these nappes include Carboniferous–Permian clastic sediments (Baumer et al. 1961; Galster et al. 2012). The Adula nappe is a possible source of the sediments deposited in a north-laying basin currently located in the aforementioned nappes. A Mesozoic cover is not observed directly on the Zervreila orthogneiss.

Variscan post-collisional (or tardi-collisional) granitoids are documented in several Alpine domains. They are particularly developed and documented in the External massifs (Bussy et al. 2000; von Raumer et al. 2009) and in the Lower Penninic basement, where this magmatism is also widely represented (Bussien et al. 2011). An age of 292 Ma for the Zervreila orthogneiss is comparable with the ages of 291 ± 4 Ma (Bussy unpublished data) and 289 ± 3 Ma (Bergomi et al. 2007) of the Verampio granite. The Antigorio granite yielded ages between 296 ± 2 and 289 ± 4 Ma (Bergomi et al. 2007). Both nappes are Lower Penninic and paleogeographically reattached to the internal Helvetic (Matasci et al. 2011). Similar granites are also found in the western Tauern Window (Eichhorn et al. 2000; Vaselá et al. 2011).

The Zervreila orthogneiss emplacement is part of the post-orogenic readjustment of the over-thickened crust (Ménard and Molnar 1988). The tectonic scenario is controlled by uplift and exhumation, which produces basins and topographic highs caused by large-scale strike slips and associated with significant concomitant magmatic activity (see the review by von Raumer et al. 2013 and references therein).

Triassic transgression and Mesozoic stratigraphy

The Mesozoic autochthonous cover of the Adula nappe exists and is coherent throughout the different outcrops (Cavargna-Sani et al. 2010; Galster et al. 2012). The presence of a pre-Triassic Verrucano-type sediment, similar to what is described in the nearby Luzzone-Terri nappe (Galster et al. 2010), was not found. The Triassic transgression (Fig. 16) is found in the Garenstock Augengneiss,

the Heinisch Stafel, and the Trescolmen Formations. The Zervreila orthogneiss perhaps did not crop out during Triassic times because no direct contact between the Triassic deposit and the Zervreila orthogneiss was noted. Triassic deposits of the Adula nappe are related to the North Penninic Triassic type (Galster et al. 2012) characterised by the typical "dolomie bicolori". Jurassic stratigraphy shows an emersion followed by a marine transgression at the end of the Jurassic (Cavargna-Sani et al. 2010; Galster et al. 2012). These data show that the Adula nappe is part of a coherent paleogeographic domain that was strongly affected by extensional tectonics during Jurassic rifting.

Implications for Alpine tectono-metamorphic evolution

The suggested Palaeozoic lithostratigraphy demonstrates the consistency of the geotectonic evolution of the northern Adula basement. This evolution implies that different pre-Mesozoic unconformities formed by pre-Alpine tectonics and stratigraphy are involved in the Alpine orogeny. The lithologic variety of the Adula basement originates clearly from the complexity of the Palaeozoic geotectonic evolution.

Supporting the consistency of the basement and cover, we do not ignore the extreme tectonic and metamorphic complexity of the Adula nappe. The geometry of the monometamorphic Zervreila orthogneiss (Fig. 2) makes obvious the intensity of the Alpine deformation.

Trommsdorff (1990) interpreted the Adula nappe as a lithospheric mélange. Furthermore, Berger et al. (2005) proposed the Adula nappe as part of a "Paleogene Tectonic Accretion Channel" (TAC, Engi et al. 2001). These models suggest a tectonic mixing during the subduction and exhumation of pieces of different paleogeographic origins. However, the northern Adula nappe cannot be considered as having been formed by a lithospheric mélange with pieces of different tectonic plates because the Adula was a consistent pre-Alpine entity. Our results suggest using a different scale to determine the kinematics that produced such a complex structure and the close imbrication of different rock types. We consider the Adula nappe as an expression of a ductile shear zone involving the entire nappe. The imbricate structure is the consequence of several phases of folding and shearing of a coherent and pre-structured pre-Alpine Adula.

Conclusions

The northern Adula nappe displays a consistent Palaeozoic geological evolution, despite severe Alpine deformation and metamorphism. The oldest formation is a Cambrian paragneiss recording bimodal magmatism (Salahorn Formation) in a back-arc geotectonic setting. The Trescolmen Formation protolith is characterised by a chaotic formation composed of marine argillaceous sediments and oceanic crust formed in a subduction-related setting with a minimum age at 460 Ma and a metamorphic age at 370 Ma. Ordovician rocks constitute both metagranitoids and a paragneiss formation. Ordovician metagranites are associated with contemporaneous mafic rocks; both rock types are calc-alkaline and emplaced in an active margin geodynamic environment. The Ordovician Heinisch Stafel Formation protolith is formed by volcanoclastic sediments. The above-mentioned formations were all involved in the Variscan orogeny and record a polyorogenic evolution. The Permian Zervreila granite intrudes these polyorogenic formations during the post-orogenic crustal readjustment of the Variscan crust (synthetic sketch of the basement lithology; see Fig. 16). The major Palaeozoic events recorded elsewhere in Alpine Palaeozoic nappes can also be traced in the northern Adula nappe.

The unconformity suggested by the entire lithostratigraphic record between pre-Variscan and younger rocks within the Adula nappe is evidence of the inheritance of pre-Alpine structures in the Adula nappe basement. The present-day structural complexity of the Adula nappe is the result of the intense Alpine ductile deformation of a pre-structured coherent entity. Mélange models for the tertiary emplacement of the Adula nappe involving an assemblage of lithological entities of different paleogeographic origins are not consistent and must be rejected.

Acknowledgments This study is supported by the Swiss National Science Foundation, Grant no. 200021_132460. We thank T. Nagel and F. Finger for their very useful comments on the manuscript. We would like to thank also L. Nicod for thin sections preparation and mounts polishing, P. Vonlanthen for support at SEM, J.-C. Lavanchy for XRF measurements and N. Hürlimann for support by glass discs LA-ICP-MS measurement. We thank F. Galster, F. Humair, H. Masson, A. Pantet, D. Schreich and A. Steck for field support and fruitful discussions. We are grateful to the Museo Cantonale di Storia Naturale for authorization to collect samples in Ticino.

References

Alonso-Perez R, Müntener O, Ulmer P (2009) Igneous garnet and amphibole fractionation in the roots of island arcs: experimental constraints on andesitic liquids. Contrib Miner Petrol 157:541–558

Arnold A, Fehr A, Jung W, Kopp J, Kupferschmid Ch, Leu W, Liszkay M, Nabholz W, Van der Plas L, Probst Ph, Wyss R (2007) Blatt 121Vals. Geologischer Atlas der Schweiz 1:25000. Swisstopo, Bern

Barbarin B (1999) A review of the relationships between granitoid types, their origins and their geodynamic environments. Lithos 46:605–626

Barboni M, Bussy F, Chiaradia M (2011) Origin of Early Carboniferous pseudo-adakites in northern Brittany (France) through massive amphibole fractionation from hydrous basalt. Terra Nova 23:1–10

Baumer A, Frey JD, Jung W, Uhr A (1961) Die Sedimentbedeckung des Gotthard-Massivs zwischen oberen Bleniotal und Lugnez. Eclogae Geol Helv 54:478–491

Berger A, Mercolli I (2006) Tectonic and Petrographic map of the Central Lepontine Alps 1:100 000 (Map sheet 43 Sopra Ceneri). Carta Geologica Speciale 127. Swisstopo, Bern

Berger A, Mercolli I, Engi M (2005) The central Lepontine Alps: notes accompanying the tectonic and petrographic map sheet Sopra Ceneri (1:100,000). Bulletin suisse de minéralogie et pétrographie 85:117–144

Bergomi MA, Tunesi A, Shi YR, Colombo A, Liu DY (2007) SHRIMP II U/Pb geochronological constraints of pre-Alpine magmatism in the Lower Penninic Units of the Ossola Valley (Western Alps, Italy). Geophysical Research Abstracts 9

Boekhout F, Spikings R, Sempere T, Chiaradia M, Ulianov A, Schaltegger U (2012) Mesozoic arc magmatism along the southern Peruvian margin during Gondwana breakup and dispersal. Lithos 146–147:48–64

Bonin B, Azzouni-Sekkal A, Bussy F, Ferrag S (1998) Alkali-calcic to alkaline post-collision granite magmatism: petrologic constraints and geodynamic settings. Lithos 45:45–70

Bussien D, Bussy F, Magna T, Masson H (2011) Timing of Palaeozoic magmatism in the Maggia and Sambuco nappes and paleogeographic implications (Central Lepontine Alps). Swiss J Geosci 104:1–29

Bussy F, Hernandez J, von Raumer JF (2000) Bimodal magmatism as a consequence of the post-collisional readjustment of the thickened Variscan continental lithosphere (Aiguilles Rouges-Mont Blanc massifs, Western Alps). In: Barbarin B, Stephens WE, Bonin B, Bouchez J, Clarke DB, Cuney M, Martin H (eds) Fourth Hutton symposium, the origin of granites and related rocks, pp 221–233

Bussy F, Péronnet V, Ulianov A, Epard JL, Von Raumer J (2011) Ordovician magmatism in the external French Alps: witness of a peri-gondwanan active continental margin. In: Gutiérrez-Marco JC, Rábano I, García-Bellido D (eds) Ordovician of the world. Cuadernos del Museo Geominero, 14. Instituto Geológico y Minero de España, Madrid, pp 75–82

Cavargna-Sani M (2008) Etude géologique et métamorphique du haut Val calanca (GR), Nappe de l'Adula. Master thesis, Université de Lausanne

Cavargna-Sani M, Epard JL, Masson H (2010) Discovery of fossils in the Adula nappe, new stratigraphic data and tectonic consequences (Central Alps). Bulletin de la Société vaudoise des Sciences naturelles 92:77–84

Cocozza T (1979) The Cambrian of Sardinia. Memorie della Società Geologica Italiana 20:163–187

Dale J, Holland TJB (2003) Geothermobarometry, P-T paths and metamorphic field gradients of high-pressure rocks from the Adula Nappe, Central Alps. J Metamorph Geol 21:813–829

Davidson J, Turner S, Handley H, Macpherson C, Dosseto A (2007) Amphibole sponge in arc crust? Geology 35:787–790

De La Roche H, Leterrier J, Grandclaude P, Marchal M (1980) A classification of volcanic and plutonic rocks using R1R2-diagram and major-element analyses—its relationships with current nomenclature. Chem Geol 29:183–210

Demathieu G, Weidmann M (1982) Les empreintes de pas de reptiles dans le Trias du Vieux Emosson (Finhaut, Valais, Suisse). Eclogae Geol Helv 75:721–757

Deutsch A (1979) Serpentinite und Rodingite der Cima Sgiu (NW Aduladecke, Ticino). Bulletin suisse de minéralogie et pétrographie 59:319–347

Egli W (1966) Geologische-perographische Untersuchungen in der NW-Aduladecke und in der Sojaschuppe (Bleniotal, Kanton Tessin). Dissertation, ETH Zürich

Eichhorn R, Loth G, Höll R, Finger F, Schermaier A, Kennedy A (2000) Multistage Variscan magmatism in the central Tauern Window (Austria) unveiled by U/Pb SHRIMP zircon data. Contrib Mineral Petrol 139:418–435

Elicki O (2006) Microbiofacies analysis of Cambrian offshore carbonates from Sardinia (Italy): environment reconstruction and developement of a drowning carbonate platform. Carnets de Géologie/Notebooks on Geology 2006:01

Engi M, Berger A, Roselle GT (2001) Role of the tectonic accretion channel in collisional orogeny. Geology 29:1143–1146

Epard JL (1989) Stratigraphie du Trias et du Lias dauphinois entre Belledonne, Aiguilles-Rouges et Mont-Blanc. Bulletin de la Societe Vaudoise des Sciences Naturelles 79:301–338

Frey JD (1967) Geologie des Greinagebiets (Val Camadra, Val Cavalasca, Val Lariciolo, Passo della Greina). Materiaux pour la Carte Geologique de la Suisse [N.S.] 131:113

Froitzheim N, Manatschal G (1996) Kinematics of Jurassic rifting, mantle exhumation, and passive-margin formation in the Austroalpine and Penninic nappes (eastern Switzerland). Geol Soc Am Bull 108:1120–1133

Galster F, Epard JL, Masson H (2010) The Soja and Luzzone-Terri nappes: discovery of a Briançonnais element below the front of the Adula nappe (NE Ticino, Central Alps). Bulletin de la Société vaudoise des Sciences naturelles 92:61–75

Galster F, Cavargna-Sani M, Epard JL, Masson H (2012) New stratigraphic data from the Lower Penninic between the Adula nappe and the Gotthard massif and consequences for the tectonics and the paleogeography of the Central Alps. Tectonophysics 579:37–55

Gansser A (1937) Der Nordrand der Tambodecke. Bulletin suisse de minéralogie et pétrographie 17:291–523

Gansser A, Pantic N (1988) Prealpine events along the eastern Insubric line (Tonale line, northern Italy). Eclogae Geol Helv 81:567–577

Gauthiez L, Bussy F, Ulianov A, Guffon Y, Sartori M (2012) Ordovician mafic magmatism in the Métailler Formation of the Mont-Fortnappe (Middle Penninic domain, western Alps)—geodynamic implications. Abstract, 9th Swiss geoscience meeting, Zürich, pp 110–111

Gebauer D (1995) A P-T-t Path for some high-pressure uItramafic/mafic rock-association and their felsic fountry-rocks based on SHRIMP-dating of magmatic and metamorphic zircon domains. Example: Central Swiss Alps. Extended abstract, 16th general meeting of IMA, Pisa, Italy, 4–9 Sept, pp 139–140

Gisler C, Hochuli PA, Ramseyer K, Bläsi H, Schlunegger F (2007) Sedimentological and palynological constraints on the basal Triassic sequence in Central Switzerland. Swiss J Geosci 100:263–272

Guillot S, Ménot RP (2009) Palaeozoic evolution of the external crystalline massifs of the Western Alps. Comptes Rendus Geosci 341:253–265

Heinrich CA (1983) Die reionale Hochdruckmetamorphose der Aduladecke, Zentralalpen, Schweiz. Dissertation, ETH, Zürich

Heinrich CA (1986) Eclogite facies regional metamorphism of hydrous mafic rocks in the Central Alpine Adula Nappe. J Petrol 27:123–154

Herwartz D, Nagel TJ, Münker C, Scherer EE, Froitzheim N (2011) Tracing two orogenic cycles in one eclogite sample by Lu-Hf garnet chronometry. Nat Geosci 4:178–183

Irvine TN, Baragar WRA (1971) A guide to the chemical classification of the common volcanic rocks. Can J Earth Sci 8:523–548

Jackson S (2008) LAMTRACE data reduction software for LA-ICP-MS. Laser ablation ICP-MS in the Earth sciences: current

practices and outstanding issues. Mineralogical Association of Canada, Short Course Series 40, pp 305–307
Jenny H, Frischknecht G, Kopp J (1923) Geologie der Adula. Materiaux pour la Carte Geologique de la Suisse [N.S.] 51:123
Koch E (1982) Mineralogie und plurifazielle Metamorphose der Pelite in der Adula-Decke (Zentralalpen). Dissertation, Universität Basel
Kündig E (1926) Beiträge zur Geologie und Petrographie der Gebirgskette zwischen Val Calanca und Misox. Schweiz Mineral Petrogr Mitt 6:3–110
Leuthold J, Müntener O, Baumgartner LP, Putlitz B, Chiaradia M (2013) A detailed geochemical study of a shallow arc-related Laccolith; the Torres del Paine Mafic Complex (Patagonia). J Petrol 54:273–303
Liati A, Gebauer D, Fanning CM (2009) Geochronological evolution of HP metamorphic rocks of the Adula nappe, Central Alps, in pre-Alpine and Alpine subduction cycles. J Geol Soc 166:797–810
Liégeois JP, Duchesne JC (1981) The Lac Cornu retrograded eclogites (Aiguilles Rouges massif, Western Alps, France): evidence of crustal origin and metasomatic alteration. Lithos 14:35–48
Liñán E, Perejón A, Sdzuy K (1993) The lower-middle Cambrian stages and stratotypes from the Iberian Peninsula: a revision. Geol Mag 130:817–833
Löw S (1987) Die tektono-metamorphe Entwicklung der Nördlichen Adula-Decke (Zentralalpen, Schweiz). Materiaux pour la Carte Geologique de la Suisse [N.S.] 161:84
Ludwig KR (2003) User's manual for Isoplot 3.00: a geochronological toolkit for microsoft excel. Berkeley Geochronology Center/ Special publication
Ludwig KR, Mundil R (2002) Extracting reliable U–Pb ages and errors from complex populations of zircons from Phanerozoic tuffs. Goldschmidt conference abstracts 2002, p 463
Maniar PD, Piccoli PM (1989) Tectonic discrimination of granitoids. Geol Soc Am Bull 101:635–643
Matasci B, Epard JL, Masson H (2011) The Teggiolo zone: a key to the HelveticûPenninic connection (stratigraphy and tectonics in the Val Bavona, Ticino, Central Alps). Swiss J Geosci 104:257–283
Mattinson JM (2005) Zircon U–Pb chemical abrasion (CA-TIMS) method: combined annealing and multi-step partial dissolution analysis for improved precision and accuracy of zircon ages. Chem Geol 220:47–66
McDonough WF, Sun SS (1995) The composition of the Earth. Chem Geol 120:223–253
Ménard G, Molnar P (1988) Collapse of a Hercynian Tibetan plateau into a late Palaeozoic European Basin and Range province. Nature 334:235–237
Meyre C, De Capitani C, Zack T, Frey M (1999) Petrology of high-pressure metapelites from the Adula Nappe (Central Alps, Switzerland). J Petrol 40:199–213
Nagel TJ (2008) Subduction, collision and exhumation recorded in the Adula nappe, central Alps. In: Siegesmund S, Fügenschuh B, Froitzheim N (eds) Tectonic aspects of the Alpine–Dinaride–Carpathian system: Geological Society, London, special publications, vol 298, pp 365–392
Nagel T, Capitani C, Frey M, Froitzheim N, Stcnitz H, Schmid SM (2002a) Structural and metamorphic evolution during rapid exhumation in the Lepontine dome (southern Simano and Adula nappes, Central Alps, Switzerland). Eclogae Geol Helv 95:301–322
Nagel T, De Capitani C, Frey M (2002b) Isograds and PT evolution in the eastern Lepontine Alps (Graubunden, Switzerland). J Metamorph Geol 20:309–324
Oberli F, Meier M, Biino GG (1994) Time constraints on the pre-Variscan magmatic/metamorphic evolution of the Gotthard and Tavetsch units derived from single-zircon U–Pb results. Bulletin suisse de minéralogie et pétrographie 74:483–488
Peacock MA (1931) Classification of igneous rock series. J Geol 39:54–67
Pearce JA (1996) A users guide to basalt discrimination diagrams. Trace element geochemistry of volcanic rocks: applications for massive sulphide exploration. Geological Association of Canada, short course notes, vol 12, pp 79–113
Pearce JA, Stern RJ (2006) Origin of back-arc basin magmas: trace element and isotope perspectives. Geophys Monogr Ser 166:63–86
Pfeifer HR, Biino G, Ménot RP, Stille P (1993) Ultramafic rocks in the pre-Mesozoic basement of the Central and External Western Alps. The pre-Mesozoic geology in the Alps. Springer, Berlin, pp 119–143
Pin C, Marini F (1993) Early Ordovician continental break-up in Variscan Europe: Nd–Sr isotope and trace element evidence from bimodal igneous associations of the Southern Massif Central, France. Lithos 29:177–196
Pleuger J, Hundenborn R, Kremer K, Babinka S, Kurz W, Jansen E, Froitzheim N (2003) Structural evolution of Adula nappe, Misox zone, and Tambo nappe in the San Bernardino area: constraints for the exhumation of the Adula eclogites. Mitteilungen der Österreichischen Geologischen Gesellschaft 94:99–122
Pupin JP (1980) Zircon and granite petrology. Contrib Miner Petrol 73:207–220
Santini L (1992) Geochemistry and geochronology of the basic rocks of the Penninic Nappes of East-Central Alps (Switzerland). Dissertation, Université de Lausanne
Schaltegger U, Gebauer D (1999) Pre-Alpine geochronology of the Central, Western and Southern Alps. Bulletin suisse de minéralogie et pétrographie 79:79–87
Schaltegger U, Gebauer D, von Quadt A (2002) The mafic-ultramafic rock association of Loderio-Biasca (lower Pennine nappes, Ticino, Switzerland): Cambrian oceanic magmatism and its bearing on early Palaeozoic paleogeography. Chem Geol 186:265–279
Schaltegger U, Abrecht J, Corfu F (2003) The Ordovician orogeny in the Alpine basement: constraints from geochronology and geochemistry in the Aar Massif (Central Alps). Bulletin suisse de minéralogie et pétrographie 83:183–239
Schmid SM, Pfiffner OA, Froitzheim N, Schönborn G, Kissling E (1996) Geophysical-geological transect and tectonic evolution of the Swiss-Italian Alps. Tectonics 15:1036–1064
Schulz B, Steenken A, Siegesmund S (2008) Geodynamic evolution of an Alpine terrane—the Austroalpine basement to the south of the Tauern Window as a part of the Adriatic Plate (eastern Alps). Geological Society, London, special publications, vol 298, pp 5–44
Spear FS (1995) Metamorphic phase equilibria and pressure-temperature-time paths. Mineralogical Society of America, Washington
Spicher A (1980) Carte tectonique de la Suisse, 1:500,000. Commission géologique Suisse. Swisstopo, Bern
Stampfli GM, Von Raumer J, Borel G (2002) A plate tectonic model for the Paleozoic and Mesozoic constrained by dynamic plate boundaries and restored synthetic oceanic isochrones. Earth Planet Sci Lett 196:17–33
Stampfli GM, Von Raumer J, Wilhem C (2011) The distribution of Gondwana-derived terranes in the Early Palaeozoic. In: Gutiérrez-Marco JC, Rábano I, García-Bellido D (eds) Ordovician of the World. Cuadernos del Museo Geominero, 14. Instituto Geológico y Minero de España, Madrid, pp 567–574

Steck A (2008) Tectonics of the Simplon massif and Lepontine gneiss dome: deformation structures due to collision between the underthrusting European plate and the Adriatic indenter. Swiss J Geosci 101:515–546

Steinmann MC (1994) Die nordpenninischen Bündnerschiefer der Zentralalpen Graubündens: Tektonik, Stratigraphie und Beckenentwicklung. Dissertation, ETH, Zürich

Sun SS, McDonough WF (1989) Chemical and isotopic systematics of oceanic basalts: implications for mantle composition and processes. Geological Society, London, special publications, vol 42, pp 313–345

Swisstopo (2012) Sheet 1254 Hinterrhein; vector dataset (used maps see http://www.swisstopo.admin.ch/internet/swisstopo/fr/home/products/maps/geology/geocover.html). Swisstopo, Bern

Trommsdorff V (1990) Metamorphism and tectonics in the Central Alps: the Alpine lithospheric mélange of Cima Lunga and Adula. Memorie della Società Geologica Italiana 45:39–49

Ulianov A, Muntener O, Schaltegger U, Bussy F (2012) The data treatment dependent variability of U–Pb zircon ages obtained using mono-collector, sector field, laser ablation ICPMS. J Anal At Spectrom 27:663–676

Van der Plas L (1959) Petrology of the northern Adula region, Switzerland. Leidse Geol Meded 24:415–598

Vaselá P, Söllner F, Finger F, Gerdes A (2011) Magmato-sedimentary Carboniferous to Jurassic evolution of the western Tauern window, Eastern Alps (constraints from U–Pb zircon dating and geochemistry). Int J Earth Sci 100:993–1027

von Raumer JF, Bussy F (2004) Mont Blanc and Aiguilles Rouges geology of their polymetamorphic basement (external massifs, Westerns Alps, France-Switzerland). Memoires de Géologie (Lausanne) 42:203

von Raumer JF, Stampfli GM, Borel G, Bussy F (2002) Organization of pre-Variscan basement areas at the North-Gondwanan margin. Int J Earth Sci 91:35–52

von Raumer JF, Bussy F, Stampfli GM (2009) The Variscan evolution in the External massifs of the Alps and place in their Variscan framework. Comptes Rendus Géosci 341:239–252

von Raumer JF, Bussy F, Schaltegger U, Schulz B, Stampfli GM (2013) Pre-Mesozoic Alpine basements—their place in the European Palaeozoic framework. Geol Soc Am Bull 125:89–108

Whalen JB, Currie KL, Chappell BW (1987) A-type granites: geochemical characteristics, discrimination and petrogenesis. Contrib Miner Petrol 95:407–419

Wiedenbeck M, Alle P, Corfu F, Griffin WL, Meier M, Oberli F, Quadt A, Roddick JC, Spiegel W (1995) Three natural zircon standards for U Th Pb, Lu Hf, trace element and REE analyses. Geostand Geoanal Res 19:1–23

Winchester JA, Floyd PA (1977) Geochemical discrimination of different magma series and their differentiation products using immobile elements. Chem Geol 20:325–343

Zulbati F (2008) Structural and metamorphic evolution of the phengite-bearing schists of the northern Adula Nappe (Central Alps, Switzerland). Geol J 43:33–57

Zulbati F (2010) Multistage metamorphism and deformation in high-pressure metabasites of the northern Adula Nappe Complex (Central Alps, Switzerland). Geol J 46:82–103